JOURNAL OF GEOPHYSICAL RESEARCH, VOL. 113, B09201, doi:10.1029/2007JB005458, 2008

On the rise of turbulent plumes: Quantitative effects of variable entrainment for submarine hydrothermal vents, terrestrial and extra terrestrial explosive volcanism

G. Carazzo,[1] E. Kaminski,[1] and S. Tait[1]

Received 22 October 2007; revised 25 May 2008; accepted 4 June 2008; published 3 September 2008.

[1] The maximum height reached by a turbulent plume rising in a stratified environment is a key tool to estimate the flux released at its source, particularly for large-scale flows because flux can often be very hard to measure directly. This height is known to be mainly controlled by the stratification of the ambient fluid, source buoyancy flux, and the efficiency of turbulent mixing between the plume and the external fluid. The latter effect has been only superficially explored in spite of its fundamental control on the dynamics. Here we show that commonly used one-dimensional models incorporating a constant entrainment coefficient do not provide satisfying predictions. We propose a new model allowing for variable entrainment which gives excellent predictions of maximum heights reached by laboratory plumes in stratified environments. We then apply our formalism to natural plumes produced by explosive volcanic eruptions under terrestrial, paleo-Martian, and Venusian conditions and by submarine hydrothermal activity at mid-ocean ridges. Source mass discharge rates deduced from maximum volcanic column heights for terrestrial eruptions are found to be greater than those estimated with the commonly used constant entrainment parameterization by a factor of 2. In the paleo-Martian atmosphere, existing models overestimate plume heights by 14–27%. In the current atmosphere of Venus, the maximum height reached by a volcanic plume is also found to be smaller than previously estimated for large eruption rates. The source heat flux released by the TAG field (Atlantic Ocean) deduced from several submarine hydrothermal plumes is found greater by a factor 3 with our model.

Citation: Carazzo, G., E. Kaminski, and S. Tait (2008), On the rise of turbulent plumes: Quantitative effects of variable entrainment for submarine hydrothermal vents, terrestrial and extra terrestrial explosive volcanism, *J. Geophys. Res.*, *113*, B09201, doi:10.1029/2007JB005458.

1. Introduction

[2] Turbulent jets and plumes play a fundamental role in a large variety of natural phenomena and industrial processes. Understanding the dynamics of plumes issuing from industrial chimneys or those generated by forest or oil fires is a major goal for environmental sciences. These large-scale plumes are able to transport toxic gas and fine particles into the high atmosphere, making the understanding of them fundamental to evaluating the energetic pollutant and particle budgets between the source and the environment [*Trentmann et al.*, 2006]. In the catastrophic case of plumes created by bombs or nuclear accidents, it is also essential to estimate the radioactive release into the atmosphere [*Manins*, 1985] and to evaluate the deposition pathways of the radioactive elements [*Chesser et al.*, 2004].

[3] In engineering, turbulent plumes are involved in building ventilation processes to supply fresh and cool air. Estimations of volume and thermal fluxes carried by turbulent plumes are therefore essential to evaluate temperature change and quality of air budgets in rooms [*Nielsen*, 1993].

[4] Quite different turbulent plumes result from the exhaust of plane and rocket reactors. These complex supersonic jets involve numerous physical phenomena including the generation of shock waves, chemical reactions and the transport of small particles [*Dash et al.*, 1985; *Sinha et al.*, 2002], but the study of the turbulence is fundamental to understanding the formation of expansion and compression waves.

[5] Famous high speed turbulent jets in nature are those produced during explosive volcanic eruptions. Volcanic eruptions produce a dense mixture of hot ash and gases that can reach altitudes of several tens of kilometers in the atmosphere or collapse to produce pyroclastic flows [*Wilson*, 1976]. The prediction of column behavior is also fundamental to evaluating climatic impacts and hazards linked to these eruptions.

[1]Equipe de Dynamique des Fluides Géologiques, IPG Paris and Université Paris-Diderot, CNRS, Paris, France.

0148-0227/08/2007JB005458$09.00

[6] Since the independent work of *Priestley and Ball* [1955] and *Morton et al.* [1956], theoretical models have been proposed to describe the physics of turbulent plumes. These models revealed that plume dynamics are mainly controlled by the efficiency of entrainment of surrounding fluid by turbulent shear at the edges of the flow. The one-dimensional steady state model by *Morton et al.* [1956] became the most used because of its powerful simplification of the treatment of the turbulence, and many authors adapted this formalism to study various specific flows, including explosive volcanic columns [*Sparks*, 1986; *Woods*, 1988], submarine hot plumes issuing from sea-floor hydrothermal vents [*Speer and Rona*, 1989; *Rudnicki and Elderfield*, 1992] or plumes of pollutants generated by industrial chimneys [*Briggs*, 1969]. Comparison of laboratory experiments on jets and plumes with the formalism of the work of *Morton et al.* [1956] showed a good agreement concerning the scaling laws governing the dynamics of these flows. One important problem solved by this approach is the prediction of the maximum height reached by a plume in a calm stratified environment. *Morton et al.* [1956] established that the maximum height depends on the source buoyancy flux, on the evolution of the background density with altitude and on the efficiency of the turbulent entrainment. Comparison between Morton et al.'s predictions and observational data of laboratory experiments [*Briggs*, 1969] validated the analytical scaling relationship between the plume height and the source thermal flux at small and large scales but the detailed quantitative predictions are not accurate.

[7] For example, in volcanology the scaling law by *Morton et al.* [1956] is particularly useful to calculate the source thermal flux liberated by past and comtemporary eruptions from the maximum column height measured or deduced from the distribution of the deposits [*Settle*, 1978; *Wilson et al.*, 1978; *Sparks*, 1986; *Carey and Sparks*, 1986; *Wilson and Walker*, 1987; *Carey and Sigurdsson*, 1989]. Recent decades have shown the development of multiphase and time-dependant numerical models to investigate several physical processes that are not accounted for in the plume model by *Morton et al.* [1956] [*Valentine and Wohletz*, 1989; *Neri and Dobran*, 1994; *Oberhuber et al.*, 1998; *Suzuki et al.*, 2005]. Other refinements were proposed, including the effect of wind [*Bursik*, 2001], variations of surrounding conditions such as tropopause height and temperature profile at different latitudes [*Glaze and Baloga*, 1996; *Caulfield and Woods*, 1998], entrainment of moist air [*Woods*, 1993], volume expansion of the entrained and heated atmospheric air [*Ishimine*, 2006, 2007], thermal disequilibrium between gas and particles [*Sparks and Wilson*, 1976], sedimentation and recycling of solid pyroclasts [*Woods and Bursik*, 1991; *Bursik et al.*, 1992; *Sparks et al.*, 1992; *Ernst et al.*, 1996; *Veitch and Woods*, 2000, 2002; *Bonadonna and Phillips*, 2003; *Folch and Felpeto*, 2005], excess pressure of the jet at the source [*Wilson et al.*, 1980; *Woods and Bower*, 1995], and additional water at the source [*Wilson et al.*, 1978]. Although numerous studies have been carried out to understand the effects of variations of environmental and source conditions on the maximum rise height, we argue that a fundamental effect, that of turbulent mixing, has not been taken into account with the same level of detailed analysis. This key ingredient is not linked to complexity of the natural environment because it has even been treated in the same simple manner when studying the simple case of a laboratory jet rising in a calm homogeneous environment whose source conditions are known.

[8] The purpose of this paper is to investigate and to quantify the contribution of the turbulent entrainment to determining the maximum height attained by a plume. For this, we begin with the one-dimensional model by *Morton et al.* [1956] to show that the quantitative predictions that can be made with the formalism in its present form do not adequately satisfy experimental data because of weaknesses in the treatment of the turbulence. We propose to incorporate into the Morton et al. formalism an improved model of variable entrainment. We have constrained this model by revisiting a large number of laboratory experiments, stretching over several decades, with the specific objective of detecting and explaining different rates of turbulent entrainment. This new model gives excellent predictions of maximum heights in stratified environments at laboratory and natural scales.

[9] The first part of this paper is devoted to improving the classical model of *Morton et al.* [1956]. In section 2 we set out the theory of *Morton et al.* [1956] on plumes rising in calm stratified environments and we test the predictions of this model on the maximum heights reached by laboratory scale plumes in section 3. In section 4, we present our alternative description of the entrainment of surrounding fluid into the plume as a function of its local buoyancy. In section 5, we apply our formalism to natural plumes created by explosive volcanic eruptions in terrestrial and extraterrestrial atmospheres. Another concrete example of source flux estimation from maximum height is also given in section 6 for plumes issuing from sea-floor hydrothermal vents at the midocean ridge in the Atlantic Ocean.

2. Theory of Turbulent Plumes

[10] The macroscopic approach introduced by *Morton et al.* [1956] is developed for a conic-shaped jet in a steady state regime in which all the dynamical variables can be averaged with altitude as "top-hat" functions. The key hypothesis by *Morton et al.* [1956] consists in a "global" representation of turbulence achieved by introducing an entrainment coefficient α_e, assumed constant, that defines the horizontal rate of entrainment of surrounding fluid (W_e) in terms of the vertical ascent rate of the jet (U),

$$W_e = \alpha_e U. \tag{1}$$

Integrated over the flow cross-section, and using the Boussinesq approximation, the three "top-hat" conservation laws of volume ($\pi Q = \pi U R^2$), momentum ($\pi M = \pi U^2 R^2$) and buoyancy ($\pi F = \pi g' U R^2$) fluxes can be written,

$$\frac{\mathrm{d}Q}{\mathrm{d}z} = 2\alpha_e M^{1/2}, \tag{2}$$

$$\frac{\mathrm{d}M}{\mathrm{d}z} = \frac{FQ}{M}, \tag{3}$$

$$\frac{dF}{dz} = -QS, \tag{4}$$

where z is the altitude and $g' = g(\rho_a - \rho)/\rho_r$ the reduced gravity with ρ_r a reference density, ρ_a the density of the ambient fluid, ρ the plume density and g the gravity. S is the stratification parameter of the environmental fluid corresponding to

$$S = -\frac{g}{\rho_r}\frac{d\rho_a}{dz}. \tag{5}$$

In this formulation of the conservation equations, the entrainment coefficient α_e is the "top-hat" coefficient, which differs from the "Gaussian" coefficient $\alpha_G = \alpha_e/2^{1/2}$ used when working with Gaussian profiles of the key variables. In a uniform environment ($S = 0$) the right hand side of equation (4) goes to zero, in which case the initial buoyancy flux is conserved with height and the set of equations (2) to (4) can be analytically solved to access the evolution of the dynamical variables with the distance from the source as a function of α_e only. In a stratified environment ($S \neq 0$), a numerical method is required to solve the set of equations.

[11] The model developed by *Morton et al.* [1956] has been extensively applied to investigate the dynamics of jets and plumes with various source conditions [*Morton*, 1959; *Bloomfield and Kerr*, 2000; *Hunt and Kaye*, 2001]. In all cases, the results strongly depend on the value of the entrainment coefficient α_e that appears indeterminable by theoretical investigations. As the dynamics are controlled by the entrainment process, laboratory experiments have been performed to determine a value for α_e that can be deduced from the opening angle of the jet. *Morton et al.* [1956] did some experiments which consisted of propelling upward a light fluid in a tank of stratified salty water. They found a constant value of $\alpha_e = 0.13$ and proposed this value as a universal constant. Decades of experimental work on turbulent plumes do not however support the assumption of a universal constant value for α_e.

[12] First experimental measurements of α_e were made on flows issuing with a negligible buoyancy [*Fischer et al.*, 1979]. Such flows are termed "pure jets" as opposed to entirely buoyancy dominated "pure plumes" which have no initial momentum. The entrainment has been found to differ between pure jets and pure plumes varying between 0.07 and 0.16 respectively [*Kaminski et al.*, 2005]. Most of the turbulent plumes that can be encountered in natural or industrial environments are "forced plumes" exiting with both buoyancy and momentum fluxes. According to the buoyancy force direction, the flow is called "negatively" or "positively" buoyant. In such flows, α_e varies between 0.05 and 0.12 according to the direction of the buoyancy force [*Chen and Rodi*, 1980; *List*, 1982; *Wang and Law*, 2002; *Kaminski et al.*, 2005]. A third term is introduced for plumes with an important deficit of initial momentum flux compared to a pure plume. This type of flow is called a "lazy plume" and α_e is found to be around 0.12 [*Morton*, 1959; *Hunt and Kaye*, 2001].

[13] Until recently, there was no theoretical explanation for the variation of α_e with buoyancy among different plumes or even within the same plume. *Kaminski et al.* [2005] developed an alternative description of the turbulent entrainment that explains these variations. In their model, the role of both positive and negative buoyancy on the entrainment process is highlighted and explicitly taken into account. The larger values of α_e in pure and lazy plumes are due to positive buoyancy which enhances the entrainment of background fluid by promoting the formation of large-scale turbulence structure. Conversely, a negative buoyancy force inhibits entrainment and reduces α_e [*Kaminski et al.*, 2005]. On the other hand, the variations within pure jets and pure plumes can be explained by the downstream evolution of each flow to a state of self-similarity [*Carazzo et al.*, 2006]. In the absence of a theory for α_e, it has become common in geophysical problems to use an arbitrary value of $\alpha_e = 0.09$ without a sound physical basis for such a choice. Here we focus on the specific problem of plume rise in a stratified environment and propose a theory that allows evaluation of the errors in the quantitative predictions induced by the use of a constant value for α_e.

3. Turbulent Plumes in a Calm Stratified Environment

3.1. Maximum Height

[14] A powerful tool provided by the approach of *Morton et al.* [1956] is the scaling law giving the maximum height reached by a plume in a calm buoyancy-stratified environment. With the aim of finding numerical solutions, *Morton et al.* [1956] introduced nondimensional parameters based on the natural length scale provided by the gradient of surrounding fluid density (S) and in particular a height scale (H_0),

$$H_0 = (2\alpha_e)^{-1/2} F_0^{1/4} S^{-3/4}, \tag{6}$$

where πF_0 is the source buoyancy flux. Solving their new set of nondimensional equations, they were able to calculate the maximum height reached by a plume (H) where the upward velocity falls to zero,

$$H = 2.57 H_0. \tag{7}$$

[15] Numerous formulae which are fundamentally variations of equation (6) have been subsequently proposed with various applications to industrial or natural plumes [*Briggs*, 1969]. With an aim of clarifying the situation and providing a general formalism, *Briggs* [1969] made a careful review of these theoretical equations and retained the following relationship,

$$H = 5 F_0^{1/4} S^{-3/4}, \tag{8}$$

which implicitly corresponds to $\alpha_e = 0.125$. *Briggs* [1969] collected heights from plumes generated by laboratory experiments [*Morton et al.*, 1956; *Crawford and Leonard*, 1962] and issuing from large oil fires [*Vehrencamp et al.*, 1955; *Davies*, 1969] to show that this simplified equation is valid for a wide range of length scales. In their review of data on turbulent plumes, *Chen and Rodi* [1980] added experimental studies to compare with the curve given by

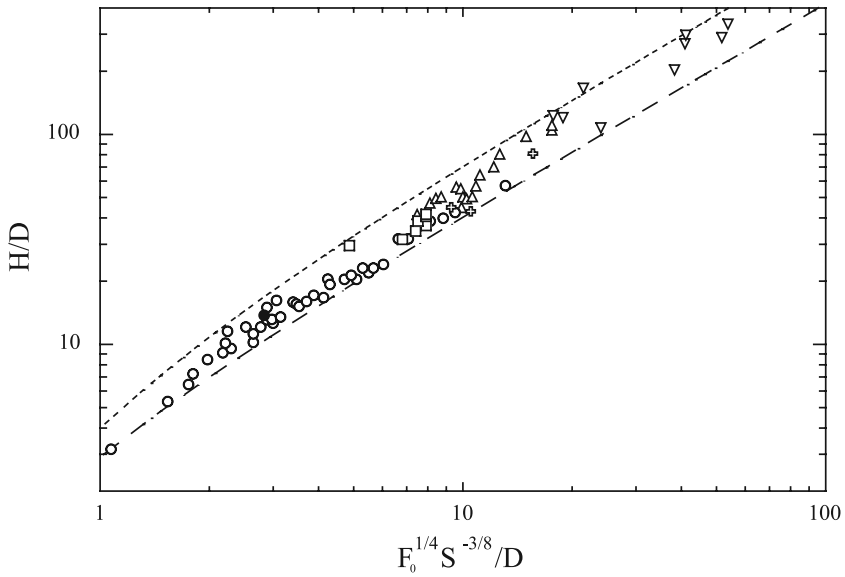

Figure 1. Rise of turbulent plumes in a calm stratified environment. Open circles: *Morton et al.* [1956]; squares: *Abraham and Eysink* [1969]; triangles: *Crawford and Leonard* [1962]; crosses: *Fan* [1967]; inverted triangles: *Fox* [1970]; solid circles: *Sneck and Brown* [1974]. Dotted and dashed lines correspond to predictions calculated with the two extreme values of α_e that can be found in the experimental literature, 0.05 and 0.16, respectively. The variables are defined in the text; D is the source diameter.

equation (8) and found a reasonable agreement although they noted an important scatter of data. Figure 1 shows indeed that the laboratory experiments reviewed by *Briggs* [1969] and *Chen and Rodi* [1980] are qualitatively consistent with the prediction of equation (8) but that a large scatter exists. For a given source buoyancy flux, the predictions of the maximum height that can be made are affected by an error of 50% while conversely the flux estimated from a given height is erroneous by one order of magnitude for large-scale plumes.

[16] Experimental errors cannot be invoked to explain this dispersion because of the robust control on the buoyancy fluxes at the source and the highly accurate measurements of maximum heights in the small scale laboratory experiments. Figure 1 shows however that all the data could potentially be explained by modifying the ratio $H/F_0^{1/4}S^{-3/4}$ for different cases, i.e., the value of α_e in equation (7). A better constraint on α_e is therefore required to examine this possibility and if proven achieve more reliable predictions.

3.2. Dilution in Forced Plumes

[17] Experimental measurements in forced plumes have shown that turbulent entrainment is limited in the near source part of the flow where inertial forces dominate compared with the buoyancy-dominated region far from the source [*Papanicolaou and List*, 1988; *Wang and Law*, 2002]. To account for this evolution, some authors proposed empirical or semi-empirical parameterizations [*Fox*, 1970; *Wang and Law*, 2002] allowing α_e to vary according to the ratio of the buoyancy and inertia forces,

$$\alpha_e = \alpha_j - (\alpha_j - \alpha_p)\left(\frac{\mathrm{Fr_p}}{\mathrm{Fr}}\right)^2, \qquad (9)$$

where $\mathrm{Fr} = U/\sqrt{|g'|R}$ is the Froude number of the jet with R the top-hat radius, U the top-hat velocity, g' the top-hat reduced acceleration due to gravity of the jet, $\mathrm{Fr_p}$ is the constant Froude number for a pure plume in a uniform environment, and α_j and α_p are arbitrary constant values of α_e for pure jets and pure plumes, respectively. *Wang and Law* [2002] applied this formalism to explain their experimental results on laboratory forced jets generated in uniform environments and found good agreement.

[18] The laboratory measurements reported in Figure 1 can be used to check the relevance of such a formulation. For this, we used equations (6) and (7) as an alternative method to determine α_e for plumes rising in a calm stratified environment. The procedure consists in determining the value of α_e which best explains each set of experimental data (Figure 2). Figure 3 shows that the values of α_e which best fit the data fall between the bounds formed by the values of α_e for pure jets and pure plumes in uniform environments [*Carazzo et al.*, 2006] except at large distances from the source where α_e values are even smaller than those predicted for a pure jet. These values clearly decrease with downstream distance from the source whereas equation (9) only predicts that α_e can increase by addition of positive buoyancy forces. The decrease of α_e has already been noticed by *Sneck and Brown* [1974] in their experiments and we show here that it is systematic.

[19] The global decrease with the distance from the source of α_e observed for plumes in a stratified environment is actually due to the ambient stratification. The source buoyancy flux that is positive falls to zero at a given height where the plume density reaches the same value as that of the ambient fluid. The flow does not stop immediately because of the momentum flux acquired during the rise. Above this height of neutral buoyancy, the flow becomes

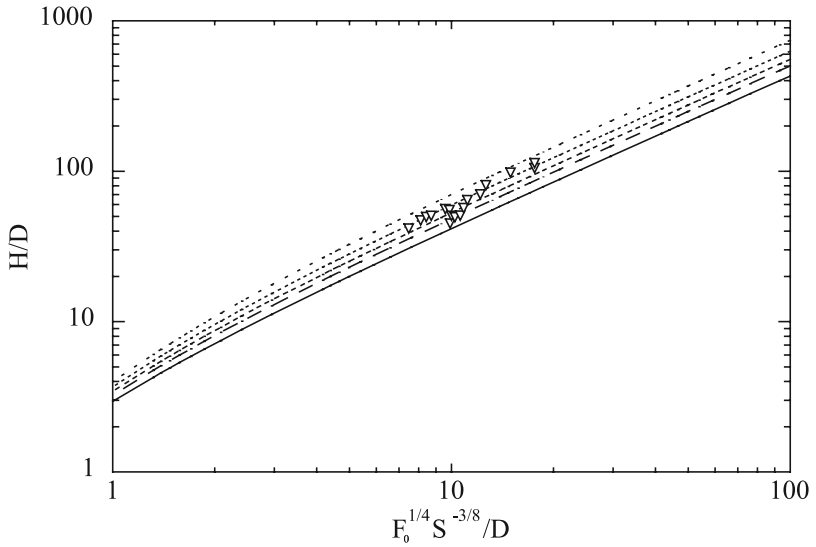

Figure 2. Example of the procedure used to determine a mean value for α_e in the laboratory experiments by *Crawford and Leonard* [1962]. The lines give the predictions for different values of α_e that are from the solid to the dotted line: 0.15, 0.13, 0.11, 0.09, 0.07, 0.05.

negatively buoyant and eventually spreads out laterally. The entrainment of surrounding fluid in this upper part is significantly reduced due to the effect of the negative buoyancy [*Kaminski et al.*, 2005]. As the thickness of the upper negatively buoyant part of the plume is a function of the source and of environmental conditions, the qualitative evolution expressed by all the points together in Figure 3 cannot be reduced to a universal law. A local model of turbulent entrainment taking into account both effects is thus required to quantitatively explain the evolution of α_e with the local buoyancy and the distance from the source.

4. An Improved Model of Turbulent Entrainment

4.1. Theory

[20] The model we use decomposes the top-hat entrainment coefficient by *Morton et al.* [1956] using the approach inspired by *Priestley and Ball* [1955]. The detailed derivation of the model are described in *Kaminski et al.* [2005] for a uniform ambient fluid, and we reproduce the main steps in Appendix A accounting for the effect of stratification in the ambient fluid. The output of the model is an expression of α_e as a function of buoyancy,

$$\alpha_e = \frac{C}{2} + \left(1 - \frac{1}{A}\right)\mathrm{Ri} + \frac{R}{2}\frac{\mathrm{d}\ln A}{\mathrm{d}z}, \tag{10}$$

where $\mathrm{Ri} = g'R/U^2$ is the Richardson number. A and C are parameters whose values depend on the shapes of the velocity, buoyancy and turbulent shear stress profiles. Assuming Gaussian profiles, A and C can be written in the compact forms,

$$A = \frac{2}{3}\left(1 + \lambda^2\right), \tag{11}$$

$$C = -6\left(1 + \lambda^2\right)\int_0^\infty r^* \exp\left(-r^{*2}\right) j(r^*)\mathrm{d}r^*, \tag{12}$$

where λ is the ratio of the characteristic $(1/e)$ width of the buoyancy profile to that of the velocity profile, j is the shape function of the turbulent shear stress profile, and $r^* = r/b_m$ with b_m a radius scale. A and C have been partially constrained by our recent analyses of the published experimental studies [*Carazzo et al.*, 2006]. The shear stress parameter C can be considered as a constant equal to 0.135, whereas the buoyancy parameter A varies with the downstream distance from the source. The evolution of A in pure jets and pure plumes at large distances from the source ($z/D > 10$) can be fitted by [*Carazzo et al.*, 2006],

$$A_j = 2.45 - 1.05\exp(-0.00465z/D), \tag{13}$$

$$A_p = 1.42 - 4.42\exp(-0.2188z/D), \tag{14}$$

where the subscripts j and p denote pure jet and pure plume respectively. To constrain the value of A_j and A_p at small distances from the source we used the laboratory measurements in uniform environments by *Baines* [1983] and *Hunt and Kaye* [2001]. These experiments involved the downward injection of a saline turbulent jet in a tank of homogeneous fresh water. At the base of the tank, fluid is drained at a known small flow rate while at the top fresh water is supplied at the same volume flux. In a steady state regime, a stratification between the fresh and the saline water initially grows and then stops, providing a means of directly estimating the volume flux in the plume at the distance from the source reached by the interface. Figure 4 shows the measurements on a pure jet and a pure plume. Theoretical models predict that the slope in such a plot is a direct function of the entrainment [*Morton et al.*, 1956; *Hunt and Kaye*, 2001] providing therefore robust con-

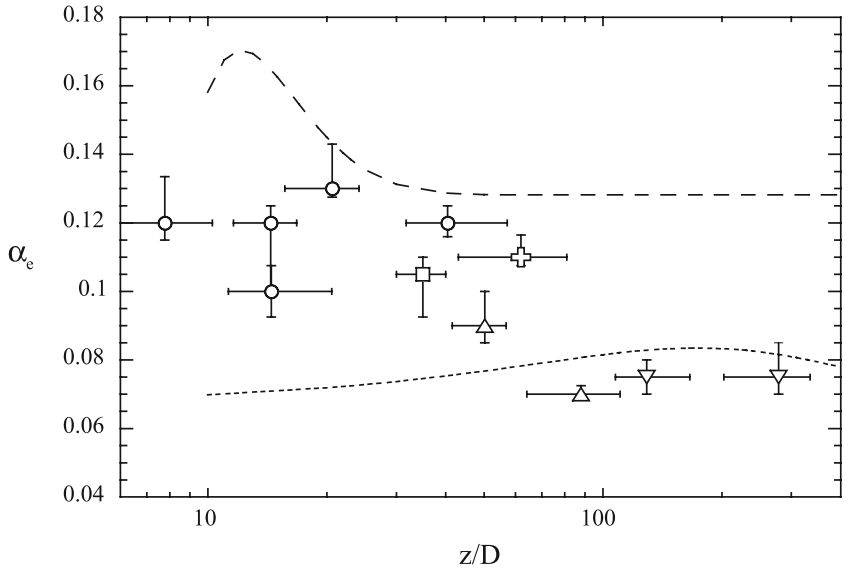

Figure 3. Evolution of the mean α_e with downstream distance from the source z/D for flows in Figure 1. The symbols are the same as in Figure 1. Dotted and dashed lines represent the evolutions of α_e for pure plumes and jets, respectively [*Carazzo et al.*, 2006].

straints on our model. To complete it, we use the following polynomial functions between $z/D = 0$ and $z/D = 10$,

$$A_j = a_1 + a_2\left(\frac{z}{D}\right) + a_3\left(\frac{z}{D}\right)^2 + a_4\left(\frac{z}{D}\right)^3, \quad (15)$$

$$A_p = b_1 + b_2\left(\frac{z}{D}\right) + b_3\left(\frac{z}{D}\right)^2 + b_4\left(\frac{z}{D}\right)^3, \quad (16)$$

where a_i and b_i are fitting parameters. With the continuity constrains of A_j, A_p, dA_j/dz and dA_p/dz at $z/D = 10$ and the reasonable hypothesis that $dA_j/dz = dA_p/dz = 0$ at the source (i.e., $a_2 = b_2 = 0$), we looked for the values of A_j and A_p at $z/D = 0$ (i.e., a_1 and b_1) which best fit the data reported in Figure 4. For pure jet, the value retained is $A_j(z/D = 0) = 1.10$ or $\lambda = 0.65$ that is consistent with our recent work on volcanic column collapse [*Carazzo et al.*, 2008], whereas for a pure plume A_p is found to be $A_p(z/D = 0) = 1.33$ or $\lambda = 1$.

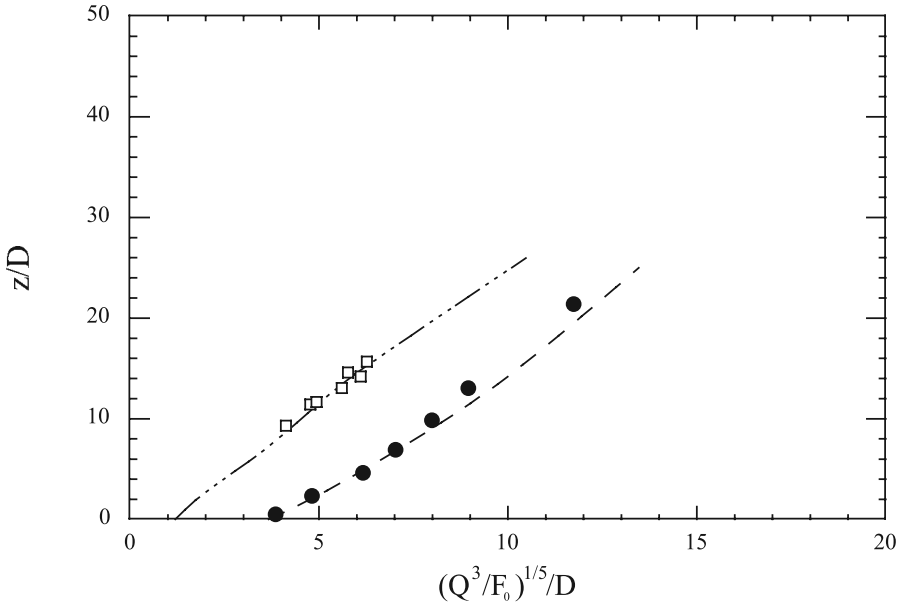

Figure 4. Laboratory measurements of volume flux with the distance from the source of a pure jet (solid circles) and a pure plume (open squares) in a uniform environment used to constrain the model at small distances from the source. The source conditions of the pure jet are $Q_0 = 2.51 \times 10^{-6}$ m^3 s^{-1}, $M_0 = 9.31 \times 10^{-7}$ m^4 s^{-2}, and $F_0 = 6.15 \times 10^{-8}$ m^4 s^{-3} [*Baines*, 1983] and for the pure plume $Q_0 = 5.44 \times 10^{-7}$ m^3 s^{-1}, $M_0 = 4.74 \times 10^{-8}$ m^4 s^{-2}, and $F_0 = 4.17 \times 10^{-7}$ m^4 s^{-3} [*Hunt and Kaye*, 2001].

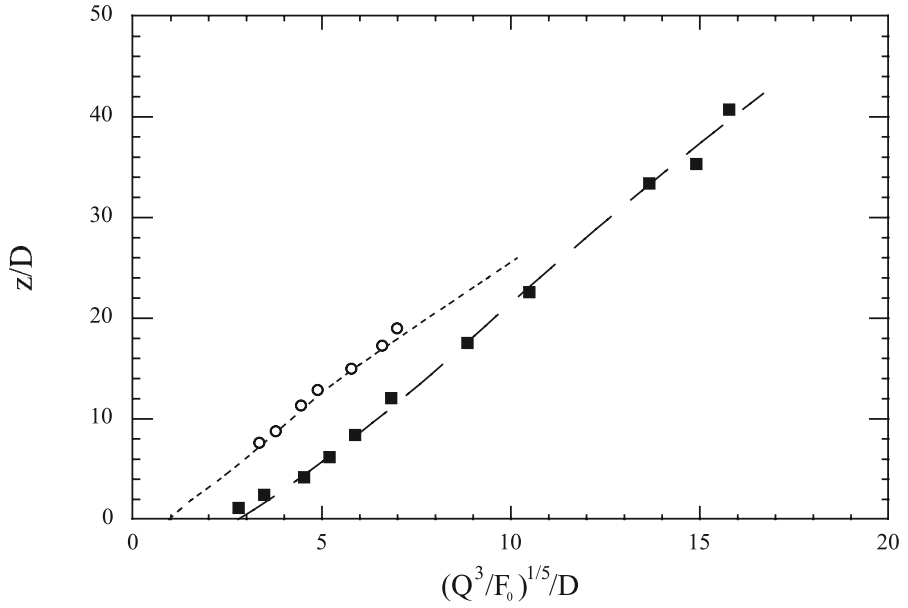

Figure 5. Predictions of the new model for laboratory measurements of volume flux in a lazy (open circles) and a forced plume (solid squares) rising in a uniform environment. The source conditions of the forced plume are $Q_0 = 2.16 \times 10^{-6}$ m^3 s^{-1}, $M_0 = 6.88 \times 10^{-7}$ m^4 s^{-2}, and $F_0 = 2.12 \times 10^{-6}$ m^4 s^{-3} [*Baines*, 1983] and for the lazy plume $Q_0 = 3.47 \times 10^{-7}$ m^3 s^{-1}, $M_0 = 1.93 \times 10^{-8}$ m^4 s^{-2}, and $F_0 = 3.41 \times 10^{-7}$ m^4 s^{-3} [*Hunt and Kaye*, 2001].

[21] Our model is now constrained for the two specific cases that are pure jets and pure plumes rising in a uniform environment. Most of the turbulent flows are nevertheless plumes with both momentum and buoyancy forces. To calculate the value of A in these common flows we use Fischer's characteristic length $L_m = \pi^{1/4}\mathrm{Ri}_0^{-1/2}R_0$ (where the subscript 0 denotes values at the source) controlling the degree of jet-like and plume-like behaviors [*Fischer et al.*, 1979]. According to the experimental results of the works of *Wang and Law* [2002] and *Papanicolaou and List* [1988], a forced plume can be considered as a pure jet at $z/L_m < 1$ and as a pure plume at $z/L_m > 5$. When $1 \leq z/L_m \leq 5$, we propose to use a first-order linear law for A,

$$A = A_j + \frac{(A_p - A_j)}{4}\left(\frac{z}{L_m} - 1\right). \qquad (17)$$

In Figure 5 we present some laboratory measurements on forced and lazy plumes generated in uniform environments by *Baines* [1983] and *Hunt and Kaye* [2001]. The excellent agreement found between our model together with equation (17) and the measurements shows that despite the simplicity of our treatment of the jet-like/plume-like behavior transition, our complete model describes well the entrainment process in this transitional region. We now investigate the predictions in the case that the local buoyancy of the plume is controlled by the environmental stratification.

4.2. Predictions of Maximum Heights in Stratified Environments

[22] To test our model with the laboratory experiments reported in Figure 1, we used data where the source and the environmental conditions are well known as only these can be used to make the quantitative test we require (Table 1).

Table 1. Experimental Data on Plumes Growing in Calm Stratified Environments

Authors	R_0 (m)	U_0 (m s^{-1})	ρ_0 (kg m^{-3})	$\rho_{a,0}$ (kg m^{-3})	S (s^{-2})	H_m/D
Hart [1961]	4.846×10^{-3}	0.725	1000	1024.58	0.102[a]	112.7
–	4.846×10^{-3}	0.307	1000	1024.61	0.066[b]	115.0
Fan [1967]	3.45×10^{-3}	0.79	1001.2	1008.7	0.245	45.0
–	1.10×10^{-3}	1.05	1004.6	1023.0	0.490	81.0
–	2.30×10^{-3}	0.50	1007.0	1024.0	0.358	43.0
Abraham and Eysink [1969]	5×10^{-3}	0.46	1000.3	1014.55	0.289	36.5
–	5×10^{-3}	0.29	1000.3	1017.30	0.230	37.0
–	5×10^{-3}	0.49	1000.5	1014.10	0.287	37.0
–	5×10^{-3}	0.54	1000.3	1013.65	0.306	28.0
–	5×10^{-3}	0.30	1000.3	1015.45	0.219	34.0
Sneck and Brown [1974]	8.89×10^{-2}	0.426	1.113	1.143	0.057	13.9

[a]Fluid stratified only between $z/D = 75.5$ and $z/D = 93.7$.
[b]Fluid stratified only between $z/D = 72.9$ and $z/D = 92.5$.

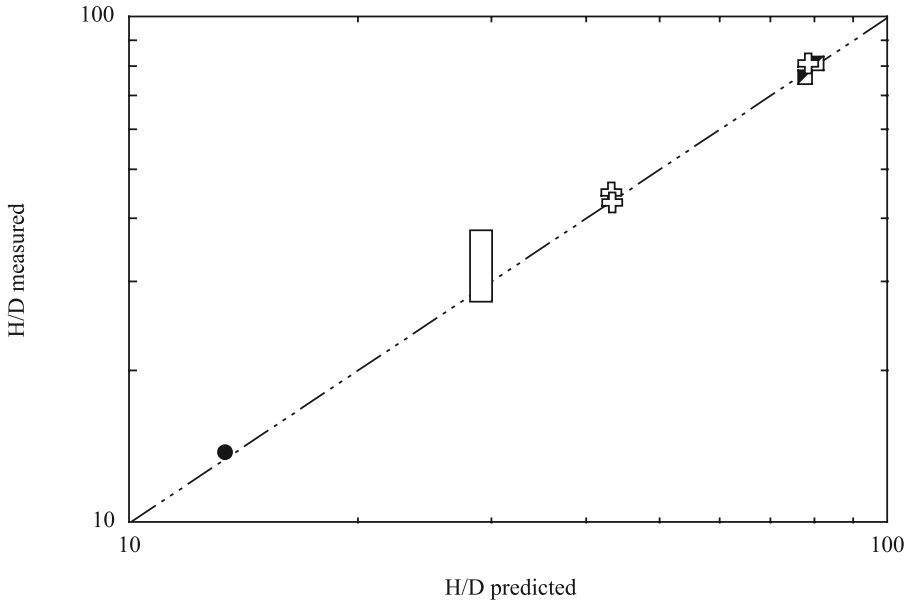

Figure 6. Predictions of the dimensionless maximum heights from our model compared with the measured heights. Black and white squares: *Hart* [1961]. The other symbols are the same as in Figure 1. Error bars correspond to the symbol sizes.

Most of these experiments involved injecting a jet of fresh water upward in a tank of salty water with density decreasing linearly with height [*Hart*, 1961; *Fan*, 1967; *Abraham and Eysink*, 1969]. *Sneck and Brown* [1974] used hot air propelled in a chamber containing thermally stratified air. We applied the variable entrainment formalism expressed by equations (10) to (17) to the Morton et al. system in equations (1) and (5). Figure 6 shows that we achieve excellent predictions of the maximum heights reached by these plumes at both small and at large distances from the source. The measurements of one study [*Abraham and Eysink*, 1969] show some scatter (Figure 6) which we think is due to the method they used to measure the maximum heights. Each of their measurements is a time-average value of the maximum height determined by recording the time history of the plume density at different heights along the plume axis and retaining the level above which the plume and ambient densities were equal. Such a procedure allows the surrounding fluid density to evolve with time and ultimately to become uniform. The maximum height reached by the plume therefore tends to increase with time becoming slightly different than the instantaneous maximum height due to the initial stratification and thus should be on average somewhat larger than our predictions as is observed in Figure 6.

[23] Our model is in excellent agreement with the small scale laboratory experiments. We propose now to apply our formalism to the very large-scale explosive volcanic eruptions in order to estimate its quantitative implications.

5. Maximum Altitude of Explosive Volcanic Plumes

5.1. Previous Studies

[24] Explosive volcanic eruptions produce the most spectacular examples of natural turbulent plumes. They can have considerable climatic impact [*Rampino and Self*, 1984; *Holasek et al.*, 1996] and effects on agriculture or health [*Hornwell*, 2007]. These high speed mixtures of hot gas and solid fragments of magma are initially heavier than the atmosphere and therefore would have a natural tendency to collapse as fountains. However, atmospheric air engulfed at the edges of the flow is heated by the solid pyroclasts and reduces the bulk density of the column to values below the ambient density. If the buoyancy inversion occurs before the initial momentum flux is exhausted, the plume becomes able to rise through the tropopause and can rise to anything up to 40 km [*Holasek et al.*, 1996] before spreading out laterally when the level of neutral buoyancy is reached. The maximum height attained by these plumes has a considerable importance because (1) it controls the transport and the dispersion of volcanic ash, gases and aerosol in the stratosphere [*Carey and Sparks*, 1986] and (2) it currently provides the only reliable estimation of mass discharge rate at the source [*Wilson et al.*, 1978]. Recent advances in real-time observations of volcanic plumes allow accurate measurements of the maximum heights attained [*Sparks et al.*, 1997]. Numerous studies comparing the scaling law and observational data on historical eruptions have shown that the thermal plume theory of *Morton et al.* [1956] can be applied to volcanic plumes and used to infer the mass flux involved during an eruption [*Settle*, 1978; *Wilson et al.*, 1978; *Sparks*, 1986; *Woods*, 1988; *Carey and Sigurdsson*, 1989; *Sparks et al.*, 1997]. The Morton et al. formalism is thus very useful to compare the energies released by two different eruptions [*Settle*, 1978] or to detect the variations of source flux during an eruption by recording plume heights [*Carey et al.*, 1990; *Holasek et al.*, 1996; *Woods*, 1998].

[25] A multitude of formulae were originally proposed to allow straightforward calculation of the source heat flux from the maximum height (Table 2). However, all these

Table 2. Relationships Between the Maximum Height Reached by a Plume and Its Initial Buoyancy Flux From the Literature[a]

Authors	H (m)	Remarks
Morton et al. [1956]	$31(1+n)^{-3/8}Q_0^{1/4}$	Q_0 thermal flux, kW
Briggs [1969]	$5F_0^{1/4}G^{-3/8}$	πF_0 buoyancy flux, $m^4 s^{-3}$
Settle [1978]	$7.89(1+n)^{-3/8}Q_0^{1/4}$	Q_0 thermal flux, cal. s^{-1}
Wilson et al. [1978]	$8.2Q_0^{1/4}$	Q_0 thermal flux, W
Sparks [1986]	$5.773(1+n)^{-3/8}(\rho_m c_p Q_0(T-T_a))^{1/4}$	Q_0 volume flux, m^3/s
Woods [1988]	$1.152\alpha^{-1/2}F_0^{1/4}G^{-3/8}$	πF_0 buoyancy flux, $m^4 s^{-3}$
Woods and Caulfield [1992]	$3.8F_0^{1/4}G^{-3/8}$	πF_0 buoyancy flux, $m^4 s^{-3}$
Sparks et al. [1997]	$5F_b^{1/4}N^{-3/4}$	F_b buoyancy flux, $m^4 s^{-3}$
Woods [1998]	$5\pi^{-1/4}Q_T^{1/4}N^{-3/4}$	Q_T enthalpy flux, J s^{-1}
Caulfield and Woods [1998]	$2.57(2\alpha_e)^{-1/2}F_s^{1/4}N_s^{-3/4}$	πF_s buoyancy flux, $m^4 s^{-3}$

[a] N and N_s are strictly equivalent to the stratification parameter S while $G^2 = S$ and $(1+n) = GT_0/(g\Gamma)$ with T_0 as the absolute temperature at the source level and Γ as the lapse rate.

scaling approaches did not include the effect of the non-uniform stratification in the terrestrial atmosphere, nor the presence of particles in the plume which liberate thermal energy. *Sparks* [1986] and then *Woods* [1988] developed models to account for these effects and compared the predictions made with the scaling law and their numerical solution of the mass, momentum and energy conservation equations in real atmospheric conditions. Their results show that for a given initial mass discharge rate, the maximum plume height predicted differs from the one predicted by the scaling laws at high latitude because of the inversion of the thermal gradient in the stratosphere. *Woods* [1995] demonstrated also that the plume height is very sensitive to the tropopause altitude which varies between tropical, intermediate and polar latitudes.

[26] The influence of environmental parameters on the maximum plume height have been extensively studied [*Woods*, 1995; *Glaze and Baloga*, 1996], in particular the effect of wind which can considerably affect the dynamics of the column [*Carey and Sparks*, 1986; *Sparks et al.*, 1997; *Bursik*, 2001; *Bonadonna et al.*, 2005]. The wind generates more ingestion of air within the plume thus reducing the maximum height, but it can also distort or cause the column to bend-over. This effect is negligible for large eruptions but becomes strong at high wind speeds and/or for low mass eruption rates [*Bursik*, 2001]. *Woods* [1993] and *Glaze et al.* [1997] demonstrated that atmospheric moisture also has an impact on the column height. In moist air, additional water vapor is entrained from the lower atmosphere into the plume and then convected to higher altitudes where it cools. When the vapor becomes saturated, condensation occurs releasing latent heat which increases thermal energy that drives the plume to higher altitudes than in a dry atmosphere.

[27] In addition, to the environmental parameters, local variations within the plume can considerably modify the maximum height. For instance, the sedimentation and reentrainment of pyroclasts are complex phenomena which are functions of the grain-size distribution, density variations within the fragments, aggregation of fine particles and wind [*Woods and Bursik*, 1991; *Bursik et al.*, 1992; *Sparks et al.*, 1992; *Ernst et al.*, 1996; *Veitch and Woods*, 2000, 2002; *Bonadonna and Phillips*, 2003; *Folch and Felpeto*, 2005]. Moreover, gradients in particle concentration within the plume can lead to partial collapse of the column [*Di Muro et al.*, 2004; *Neri et al.*, 2007].

[28] Since the pioneering works of *Settle* [1978] and *Wilson et al.* [1978], numerous factors controlling the volcanic plume behavior have thus been identified. However, despite the important improvements that were added into the theoretical framework of *Morton et al.* [1956] to develop a model for volcanic plumes, quantitative predictions remain strongly controlled by the parameterization of the turbulent entrainment, i.e., of α_e. In the face of the range of experimental measurements of α_e in the literature it has been common to use a mean value of 0.09 for volcanic plumes. This choice might be motivated by averaging the two extreme values found in the literature so as to account for the evolution of a volcanic column from a jet-like behavior at its base where the entrainment is low to a plume-like behavior in the upper part where entrainment is more important. This choice for α_e is nevertheless somewhat arbitrary and legitimately leads us to consider the generality of this value and check if first order effects induced by the evolution of α_e in a volcanic plume may have been neglected by taking α_e to be constant equal to 0.09. We therefore compare quantitative predictions made with $\alpha_e = 0.09$ and with variable α_e. For this we go back to the simple case of a steady state plume loaded with sufficiently fine particles to consider no sedimentation and complete thermal equilibrium between the two phases rising in a calm dry atmosphere as in the reference model of *Woods* [1988].

5.2. On Earth

[29] To apply Morton et al.'s formalism to volcanic eruptions, we used the method of *Woods* [1988] in which the evolution of the mixture density with altitude is given by the mixture temperature calculated using the conservation equation of energy. To compare the source mass discharge rate estimated from the column height with the classical method and with our model, we used $\alpha_e = 0.09$ and our formalism on an ensemble of well studied eruptions (Table 3). Figure 7 shows that we predict a higher mass discharge rate for given column height with a systematic scatter corresponding to a factor of 2. This implies that the average α_e is larger than 0.09. This is due to more efficient turbulent entrainment in the buoyant part of the plume. This also means that bulk entrainment is not much affected by reduced entrainment at the base of the negatively buoyant column, which agrees with the analytical predictions by

Table 3. Source and Environmental Parameters of Some Well Known Eruptions[a]

Eruption	Altitude (m)	Atmospheric Profile	T_{ext} (K)	T_0 (K)	x_0 (wt%)	Plume Height (km)	Reference
Cerro Negro (1992)	675	tropical	300	1200	3–4	7.5	(1–3)
Mt. St. Helens (B1)	3000	intermediate	268	1200	2.3	15.4	(4–6)
Mt. St. Helens (B2)	3000	intermediate	268	1200	2.3	17.5	(4–6)
Mt. St. Helens (B4)	3000	intermediate	268	1200	2.3	19.0	(4–6)
Pinatubo (C1)	1745	tropical	293	1200	2.7	21.0	(7–9)
El Chichon (A)	1150	tropical	296	1120	3.3	~17	(10–12)
El Chichon (B)	1150	tropical	296	1120	3.3	~17	(10–12)
El Chichon (C)	1150	tropical	296	1120	3.3	~17	(10–12)

[a]T_{ext}, T_0, and x_0 are the atmospheric temperature, the magmatic temperature, and the amount of gas in the mixture at the source, respectively. Exit velocities are assumed sonic after decompression and therefore are a direct function of the amount of gas [*Woods and Bower*, 1995]. x_0 is calculated by assuming a total exsolution of volatiles and then corrected for the presence of lithics and crystals. Radar measurements of column heights are favored in comparison to estimations from the distribution of the deposits because of the hypotheses on the entrainment inherent in these models [*Carey and Sparks*, 1986]. Sources: 1, *Roggensack et al.* [1997]; 2, *Connor et al.* [1993]; 3, *Wallace* [2005]; 4, *Carey et al.* [1990]; 5, *Rutherford et al.* [1985]; 6, *Carey and Sigurdsson* [1985]; 7, *Holasek et al.* [1996]; 8, *Koyaguchi and Ohno* [2001]; 9, *Borisova et al.* [2005]; 10, *Luhr* [1990]; 11, *Sigurdsson et al.* [1987]; 12, *Varekamp et al.* [1984].

Hunt and Kaye [2001]. One can note that this difference is mainly due to the term involving C in equation (10) that ensures a minimum of entrainment and the term containing Ri that counts for 40% in the estimated height. The third term in equation (10) affects the estimated height by only a few percent. The predictions of our model provide new formulae for determining mass discharge rate feeding a volcanic column from its maximum height. For this, we considered andesitic magma with an initial temperature of 1200 K and a density of 2400 kg m^{-3}. The specific heat of the volcanic gas (H_2O) and solid particles are 2000 J kg^{-1} K^{-1} and 1050 J kg^{-1} K^{-1} [*Neuville et al.*, 1993], respectively. We consider an initial velocity of 300 m s^{-1} consistent with 5wt% of gas in the mixture [*Woods and Bower*, 1995]. These initial conditions are input into the model by *Woods* [1988] but with our description of variable entrainment rather than constant α_e, and the maximum plume heights corresponding to different mass discharge rates are then calculated by increasing the vent diameter. We consider polar, intermediate and tropical atmospheres (Figure 8). Figure 9 shows the source mass discharge rate predicted for given column height with our model. On the basis of these predictions, we propose in Table 4 a set of relations between the mass discharge rate feeding a volcanic column and its maximum height measured either by radar or deduced from the distribution of the deposits [*Koyaguchi and Ohno*, 2001].

[30] We now examine the entrainment in volcanic plumes rising in quite different atmospheric conditions on other telluric planets for which there is even less reason to suppose that a constant value of 0.09 should be valid.

5.3. On Mars

[31] Explosive volcanism probably occurred during the past history of Mars, and many authors proposed to explain some morphological particularities and radar measurements at the surface by the presence of volcanic ash and pyroclastic flow deposits from explosive activity [*Hort and Weitz*,

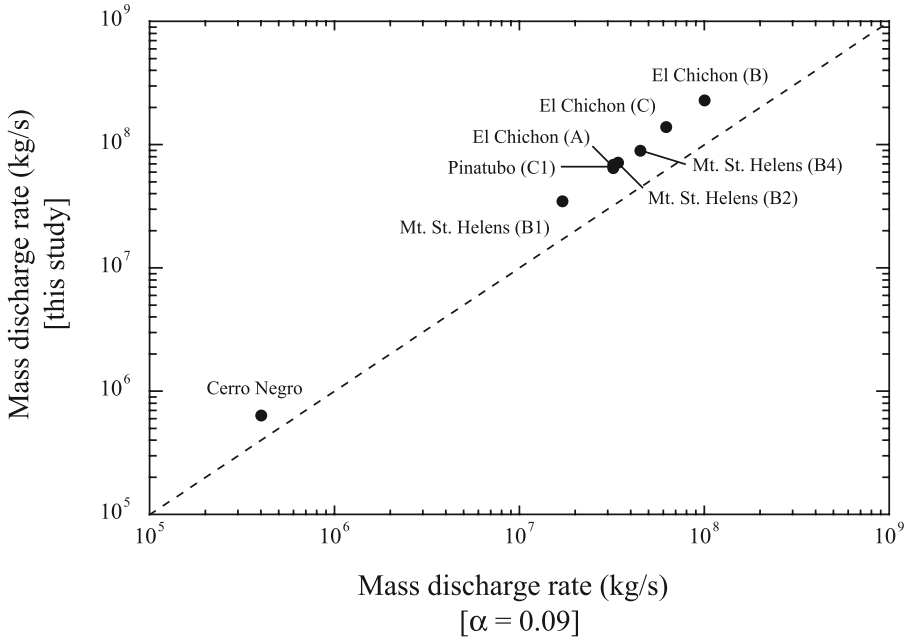

Figure 7. Comparison of the predictions of mass discharge rate with the model of *Woods* [1988] using $\alpha_e = 0.09$ and the variable entrainment law on an ensemble of well-studied Plinian columns.

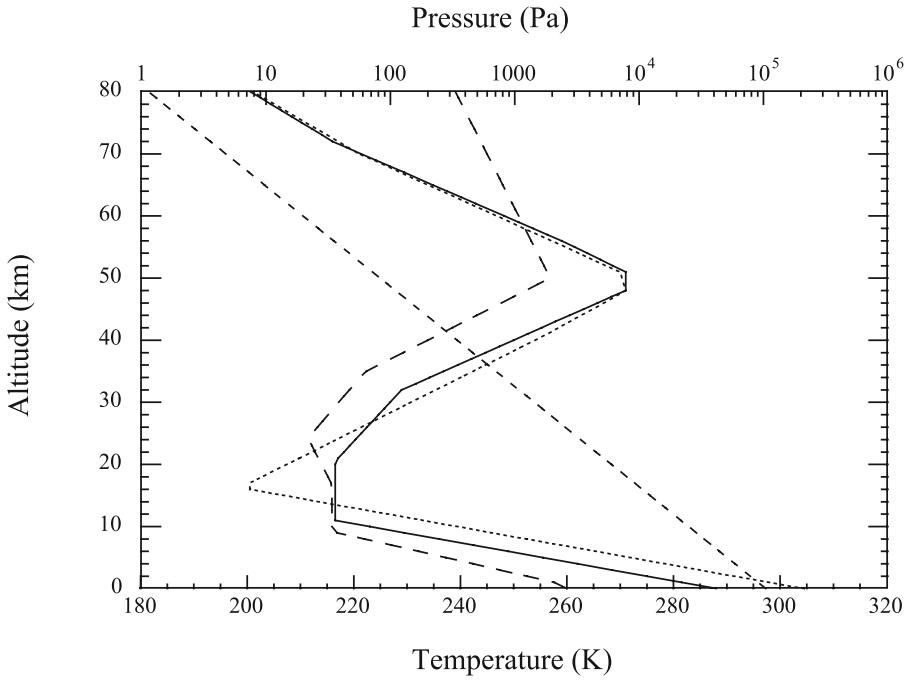

Figure 8. Temperature and pressure (dashed line) profiles in the terrestrial atmosphere at polar (long dashed line), intermediate (solid line), and tropical (dotted line) latitudes.

2001]. The current conditions on Mars strongly differ from those on Earth and would considerably modify the dynamics of volcanic plumes. Theoretical models were therefore elaborated to study the effect of this extreme environment [*Wilson and Head*, 1994; *Kusanagi and Matsui*, 2000; *Hort and Weitz*, 2001; *Glaze and Baloga*, 2002].

[32] The low gravity (3.7 m s^{-2}) and low pressure (10^3 Pa) at the surface of Mars should have two major effects on volcanic column behavior. First, the fragmentation of the magma may be enhanced compared with the Earth [*Wilson and Head*, 1994]. The volcanic products are expected to be finer-grained than those on Earth and therefore plausibly would remain in the column up to the maximum height. Secondly, the low atmospheric density may to first order promote the formation of high buoyant plumes. Many authors have proposed indeed that under the current conditions of Mars, a volcanic plume would reach altitudes greater than 100 km [*Wilson and Head*, 1994; *Kusanagi and*

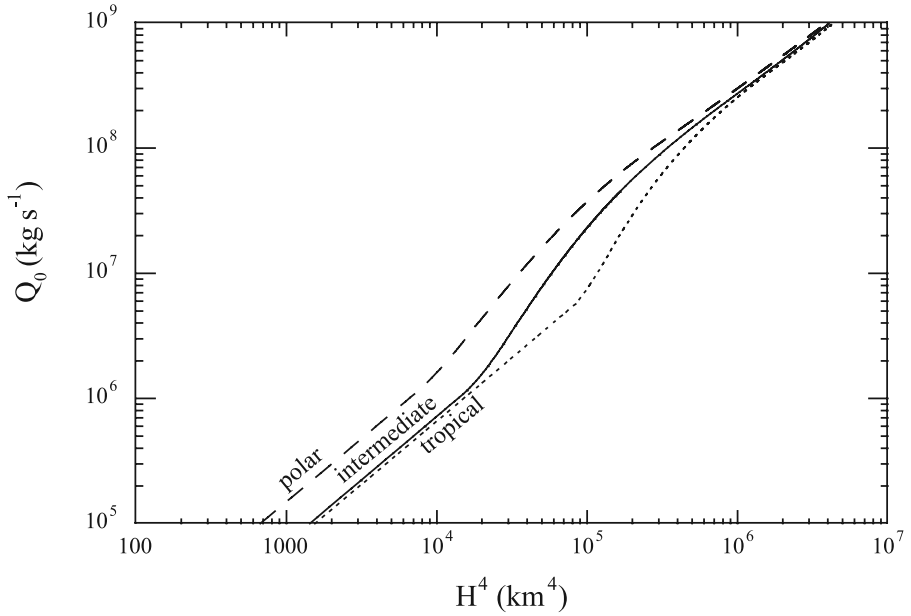

Figure 9. Source mass discharge rate as a function of the maximum height to the fourth power. Magma properties and source conditions are given in the text. Dashed, solid, and dotted lines give the predictions made with our model for polar, intermediate, and tropical atmospheric conditions, respectively.

Table 4. Relations Between the Source Mass Discharge Rate (Q_0) Feeding a Volcanic Column and Its Maximum Measured Height (H) for Polar, Intermediate, and Tropical Atmospheric Conditions[a]

Conditions	$Q_0 = aH^4 + b$	
Polar, $H < 10$ km	$a = 156$	$b = 0$
Polar, 10 km $< H <$ 23 km	$a = 244$	$b = -5.3 \times 10^7$
Polar, $H > 23$ km	$a = 386$	$b = -2.3 \times 10^6$
Intermediate, $H < 12$ km	$a = 74$	$b = 0$
Intermediate, 12 km $< H <$ 17 km	$a = 258$	$b = -4.6 \times 10^6$
Intermediate, $H > 17$ km	$a = 252$	$b = 0$
Tropical, $H < 18$ km	$a = 70$	$b = 0$
Tropical, 18 km $< H <$ 25 km	$a = 278$	$b = -2.5 \times 10^7$
Tropical, $H > 25$ km	$a = 234$	$b = 0$

[a] Q_0 is in kg s^{-1}, H in km, a in kg s^{-1} km^{-4} and b in kg s^{-1}.

Matsui, 2000; *Hort and Weitz*, 2001]. *Glaze and Baloga* [2002] re-examined these estimations by investigating the limits of validity of the Morton et al. model in the Martian environment. They demonstrated that the low atmospheric pressure implies that some basic assumptions required to apply the convective model are no longer valid. *Glaze and Baloga* [2002] gave a minimum plausible limit for plume height on Mars by applying their model up to 9 km height, below which the model should not breakdown.

[33] An interesting alternative way to study the behavior of volcanic plumes on Mars consists in considering an early Mars atmosphere with a higher surface pressure [*Hort and Weitz*, 2001; *Glaze and Baloga*, 2002]. The current atmosphere of Mars has been measured by the Viking and Mars Pathfinder missions which gave consistent results slightly differing because of seasonal variations [*Hort and Weitz*, 2001]. The paleotemperature and pressure profiles we use (Figure 10) are those retained by *Glaze and Baloga* [2002]. The surface pressure is assumed to be of the same order of magnitude as currently on Earth while the surface temperature is taken equal to the current surface temperature as suggested by *Squyres and Kasting* [1994]. The past composition of the Martian atmosphere is assumed identical to the contemporary composition with mainly CO_2 and some N_2, Ar and O_2 [*Seiff and Kirk*, 1977] with a bulk gas constant of 191 J K^{-1} kg^{-1}.

[34] The rheology of the magma on Mars cannot be constrained with actual geological data. In their model of conduit flow, *Hort and Weitz* [2001] considered the two end-member cases that are basaltic and rhyolitic composition and showed that the free decompression velocities are in the range of 100–600 m s^{-1} mainly depending on the initial gas content and independent of the composition of the magma. For our calculations we take a magma at 1000 K with a gas mass fraction of 5wt% (H_2O) which implies a velocity of 600 m s^{-1} [*Hort and Weitz*, 2001]. The properties of the eruptive mixture are the same as those used for the terrestrial case. We used these source conditions to calculate the maximum plume heights for different eruption rates by increasing the vent radius within the limits of validity of the model established by *Glaze and Baloga* [2002] for the Martian paleoenvironment (initial eruption rate less than 1.4×10^9 kg s^{-1}).

[35] Figure 11 shows that the use of a constant value of $\alpha_e = 0.09$ [*Hort and Weitz*, 2001] leads to a 14–27% overestimation of plume heights. As *Hort and Weitz* [2001] demonstrated that the maximum plume heights on Mars are slightly dependent on the composition of the magma and nearly independent of the volatile content, this shows that turbulent entrainment is the first order parameter of quantitative predictions. Most accurate quantitative predictions would certainly be achieved by including our description of

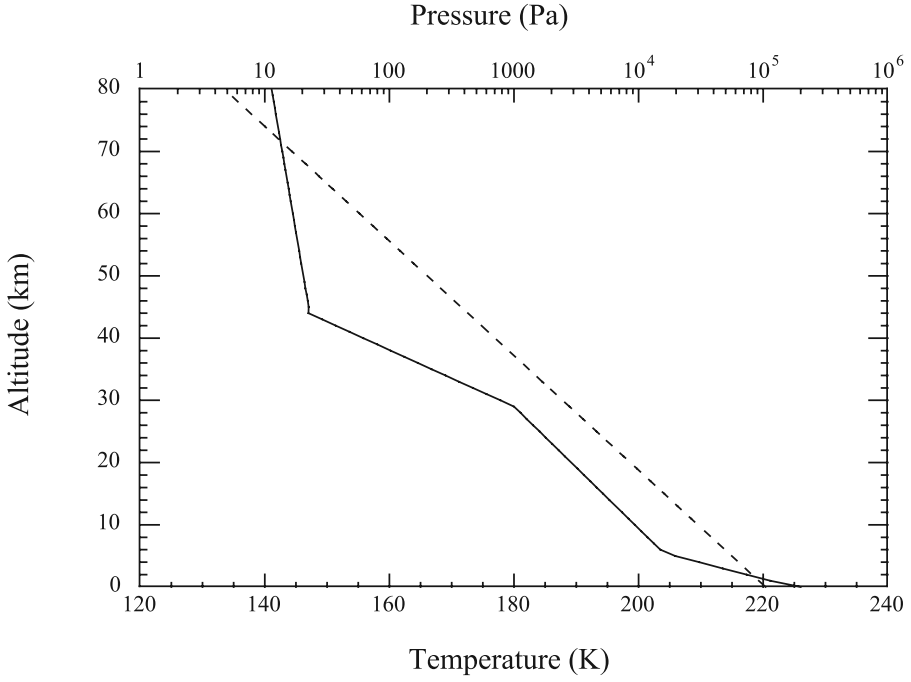

Figure 10. Temperature (solid line) and pressure (dashed line) profiles of the paleo-martian atmosphere [*Glaze and Baloga*, 2002].

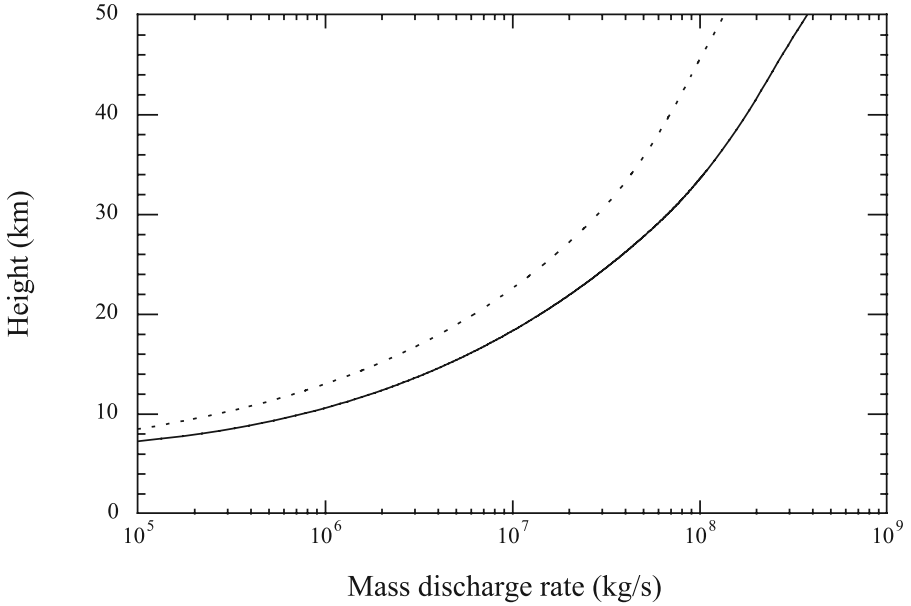

Figure 11. Prediction of maximum height reached by a volcanic plume in the early atmosphere of Mars as a function of the source mass discharge rate. Dotted and solid lines correspond to predictions with α_e = 0.09 and our model, respectively.

the turbulent entrainment in a multicomponent model [*Hort and Weitz*, 2001; *Glaze and Baloga*, 2002].

5.4. On Venus

[36] High concentrations of SO_2 detected at the top of the Venusian atmosphere by the Pioneer Venus orbiter suggest that explosive activity is currently occurring on the planet [*Esposito*, 1984]. As on Mars, some morphological evidence and radar measurements have been invoked to prove the existence of past or current explosive volcanic eruptions [*Robinson et al.*, 1995]. The extreme atmospheric conditions on Venus raise the question of whether transport of SO_2 by explosive volcanic plumes up to high altitudes (70 km) is possible [*Thornhill*, 1993]. The high atmospheric pressure (9 MPa in the lowlands) inhibits the exsolution of volatiles from the magma inducing lower ejection velocities than on Earth [*Wilson and Head*, 1983]. Moreover, the high temperature at the surface (750 K) reduces the relative density difference between the volcanic mixture and the environment. Both effects may promote the formation of pyroclastic fountains rather than high convective columns.

[37] Previous numerical models [*Kieffer*, 1995] and theoretical studies [*Thornhill*, 1993; *Robinson et al.*, 1995; *Glaze*, 1999] were elaborated to understand whether a buoyant volcanic plume could emerge in such an environment. For comparison with the results of *Robinson et al.* [1995] and *Glaze* [1999], we consider a volcanic mixture at 1400 K with an initial gas mass fraction of 5wt% (H_2O) implying an initial velocity of 270 m s^{-1} [*Wilson and Head*, 1983] and we use the thermal structure and pressure gradient of the Venusian atmosphere given in Figure 12. The gas constant and specific heat for the bulk atmosphere are 191 J kg^{-1} K^{-1} and 835 J kg^{-1} K^{-1} respectively [*Glaze*, 1999].

[38] Figure 13 shows the results of *Robinson et al.* [1995] and *Glaze* [1999] who calculated the maximum heights of plumes erupting from Maat Mons, a 9 km high volcano. For large mass fluxes, the results of the work of *Robinson et al.* [1995] are lower than those of *Glaze* [1999] because of the method used to determine the plume heights. *Robinson et al.* [1995] considered surface atmospheric conditions at the vent and added the vent elevation to the final plume heights while at 9 km height atmospheric pressure is in reality much lower than at the surface providing greater buoyancy to the plume as pointed out by *Glaze* [1999]. However, it appears that other differences between those models partly compensate for the effect of differing source conditions leading to only slightly different results between the two studies.

[39] As we use a one component model, we calculated the maximum heights of plumes issuing from vent radii ranging from 20 m to 300 m in the same conditions as *Robinson et al.* [1995]. Figure 13 shows that for small mass fluxes our results are similar to those of *Robinson et al.* [1995], whereas for large mass fluxes the two predictions diverge. In the light of our results, the plume heights predicted by *Glaze* [1999] are probably too high. Accounting for their corrections, we expect that plumes erupting from a vent 300 m in radius are only able to reach 50 km. In accordance with previous studies, volcanic plumes on Venus are unable to reach 70 km [*Thornhill*, 1993; *Robinson et al.*, 1995; *Glaze*, 1999] and other mechanisms must be invoked to explain the high concentrations of SO_2 in the high Venusian atmosphere, such as additional volatiles [*Thornhill*, 1993] or high atmospheric convection cells [*Esposito*, 1984].

6. Application to Black Smokers

[40] Here we apply our model of entrainment to submarine plumes rising from hydrothermal vents at mid-ocean ridges. These plumes, born from the interaction between the oceanic crust and ocean water that has percolated down, have been extensively studied because of their important

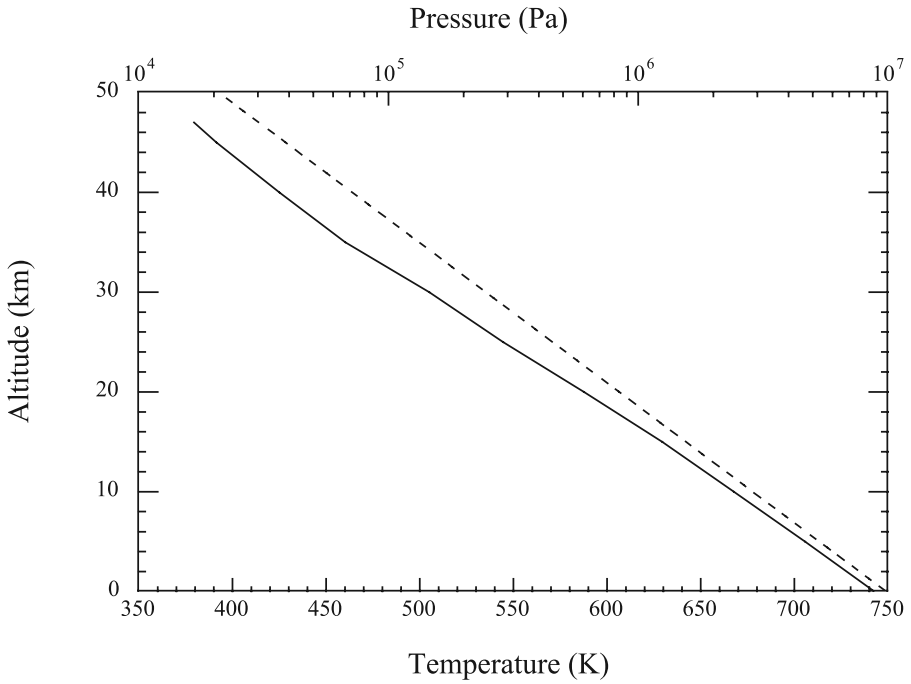

Figure 12. Temperature (solid line) and pressure (dashed line) profiles of the current Venusian atmosphere [*Glaze*, 1999].

contribution to the global energetic budget of Earth and chemical balance of oceans [see *Ramondenc et al.*, 2006, for a review]. The great depths of black smoker vents and the high temperatures of the flow make it difficult to directly measure the heat flux liberated and only minimal data exist [*Ramondenc et al.*, 2006]. An alternative method consists in detecting the heights of neutral buoyancy of submarine plumes at which they spread out laterally and then estimating the source heat fluxes with a model for turbulent convective plumes. *Rudnicki and Elderfield* [1992] applied this method to five plumes found in the TAG hydrothermal field at 26°N on the Mid-Atlantic Ridge.

[41] A plume of given composition is quickly modified by engulfing different levels of environmental seawater.

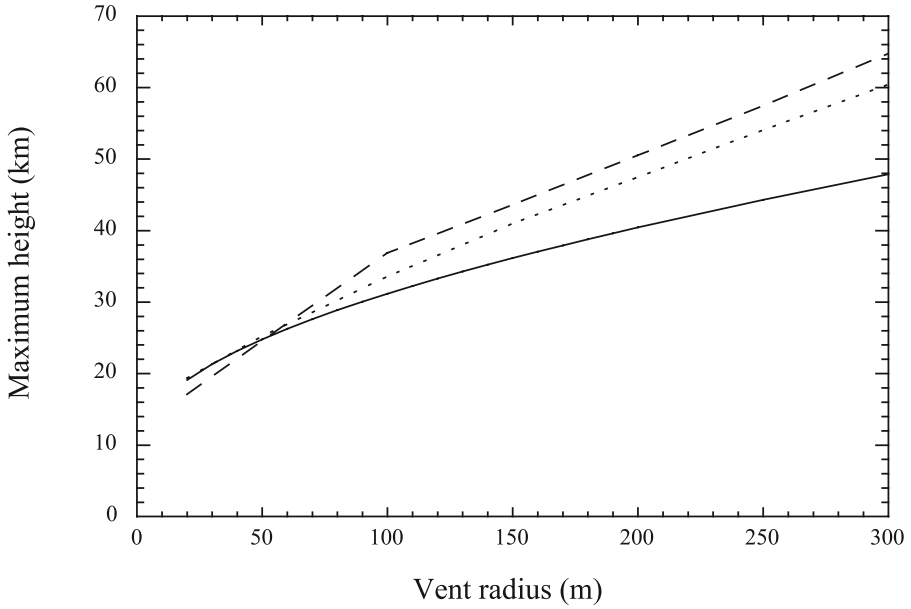

Figure 13. Prediction of maximum height reached by a volcanic plume on Venus as a function of the vent radius. Dashed, dotted, and solid lines correspond to the results of *Glaze* [1999], *Robinson et al.* [1995], and our predictions, respectively.

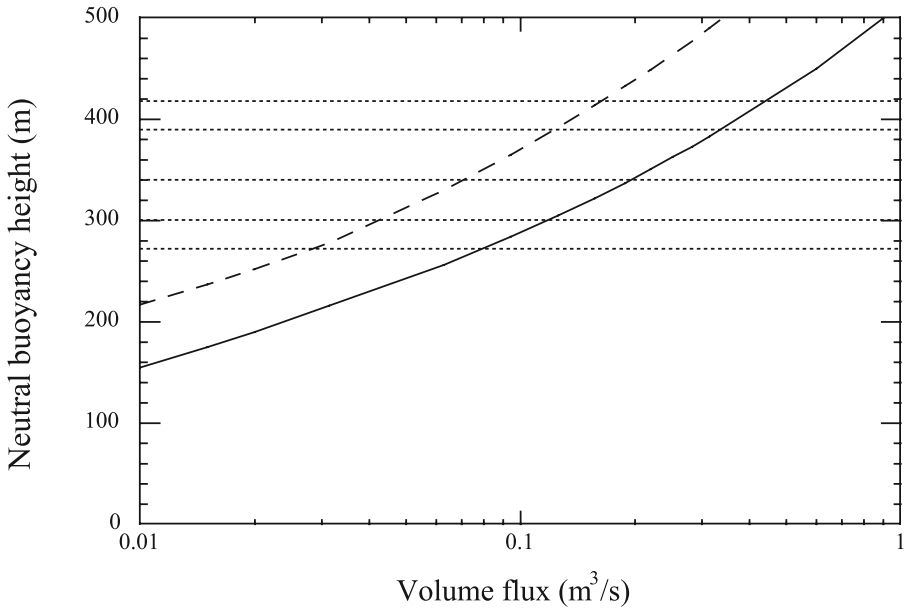

Figure 14. Neutral buoyancy height reached by hydrothermal plumes as a function of the source volume flux. Dashed line gives the prediction of *Rudnicki and Elderfield* [1992], whereas the solid line corresponds to our calculation. Dotted lines give the neutral buoyancy heights of the five plumes detected by *Rudnicki and Elderfield* [1992].

Speer and Rona [1989] adapted the model of *Morton et al.* [1956] to include the effects of temperature and salinity changes with depth in order to estimate the heights of submarine plumes in the Pacific Ocean and the Atlantic Ocean for given source heat fluxes. *Rudnicki and Elderfield* [1992] used their model to calculate the heat fluxes emitted by a large plume detected by Mn concentration measurements at mid-ridge in the Atlantic Ocean. This plume is characterized by five levels of neutral buoyancy corresponding to five plumes issuing from multiple sources of hydrothermal fluid on the TAG mound. For this study, we used their model of a submarine plume described in Appendix B. The environmental conditions are calculated with the equation of state of seawater providing the seawater density as a function of the salinity, the temperature and the pressure. The Atlantic temperature and salinity gradient profiles are $dT/dz = 5.4 \times 10^{-4}$ K m^{-1} and $dS_a/dz = 3.7 \times 10^{-5}$ m^{-1} [*Rudnicki and Elderfield*, 1992]. The source conditions of the hydrothermal plumes having been measured by submersible operations and the temperature can be taken equal to 360°C [*Rudnicki and Elderfield*, 1992] while the salinity is 34.923‰ [*Speer and Rona*, 1989].

[42] The neutral buoyancy heights of the plumes measured by *Rudnicki and Elderfield* [1992] are between 3200 m and 3450 m depth. The TAG field being located at 3640 m depth, the plumes reached their point of buoyancy inversion between 200 m and 400 m height. Figure 14 shows the estimates of volume fluxes that can be made by using the model of *Rudnicki and Elderfield* [1992] and with our model of entrainment. The heat fluxes can be calculated by using the heat capacity of the bulk hydrothermal fluid, $c_p = 6400$ J kg^{-1} K^{-1} [*Bischoff and Rosenbauer*, 1985; *Lupton et al.*, 1989]. Our estimation of the total heat flux is three times greater than that by *Rudnicki and Elderfield* [1992] (Table 5). This disagreement entirely lies in the description of the turbulence because the plume is considered like a jet with a small α_e by *Rudnicki and Elderfield* [1992] while in reality the plume should follow the same evolution as the laboratory experiments described in section 4.2.

7. Conclusion

[43] We have shown that the model of *Morton et al.* [1956] in its original form is not sufficient to explain all the experimental data that can be found in the literature. We proposed an improved description of the turbulent entrainment that varies as a function of buoyancy. The model is validated by laboratory experiments in uniform environments and is shown to predict maximum plume heights in calm stratified environments with good accuracy. For large-scale explosive volcanic plumes the classical predictions made with α_e a constant equal to 0.09 give acceptable results in terrestrial conditions but with a systematic error of a factor 2 on the estimate of fluxes. In the extreme atmospheric conditions on other telluric planets the turbulent entrainment is nevertheless increased which induces lower column heights than predicted by models with α_e =

Table 5. Estimations of the Total Heat Flux Liberated by the High-Temperature Plumes With a Constant α_e [*Rudnicki and Elderfield*, 1992] and With Our Model

Plume Height (m)	Heat Flux (MW), α_e cst	Heat Flux (MW), This Study
420	360	1104
390	267	816
340	159	468
300	94	283
270	63	182
Total	943	2853

0.09. In the paleo-Martian atmosphere, previous studies overestimated the plume heights by about 14–27%. On Venus, volcanic plumes are unable to reach the high atmosphere and our model predicts even lower altitudes compared with the estimations of previous studies. The parameterization of the entrainment that we used is universal and can therefore be used for other applications such as sea-floor hydrothermal plumes. Our results suggest that studies of sea-floor heat budgets based on a constant α_e plume models may substantially underestimate the heat flux.

Appendix A: Theoretical Model of Entrainment in a Stratified Environment

[44] We extend here the model of entrainment presented in *Kaminski et al.* [2005] for a density-stratified environmental fluid. Considering a ring-shaped volume of air, in Boussinesq approximation and steady state, the mass and momentum conservation laws can be written,

$$\frac{\partial}{\partial z}(r\overline{w}) + \frac{\partial}{\partial r}(r\overline{u}) = 0, \tag{A1}$$

$$\frac{\partial}{\partial z}\left(r\overline{w}^2\right) + \frac{\partial}{\partial r}(r\overline{uw}) = r\overline{g'} - \frac{\partial}{\partial r}\left(r\overline{\tilde{u}\tilde{w}}\right), \tag{A2}$$

$$\frac{\partial}{\partial z}(r\overline{wg'}) + \frac{\partial}{\partial r}(r\overline{ug'}) = -r\overline{w}\frac{\mathrm{d}\rho_a}{\mathrm{d}z}\frac{g}{\rho_r}, \tag{A3}$$

where r is the distance from the axis and $\overline{\tilde{u}\tilde{w}}$ is the turbulent shear stress. Over-bars denote Reynolds-averaged values for radial velocity $\overline{u}$, vertical velocity $\overline{w}$ and reduced gravity $\overline{g'}$.

[45] From the mass and momentum conservation equations, one can derive the conservation equation of kinetic energy of axial mean motion,

$$\frac{\partial}{\partial z}\left(\frac{1}{2}r\overline{w}^3\right) + \frac{\partial}{\partial r}\left(\frac{1}{2}r\overline{u}\overline{w}^2\right) = r\overline{w}\overline{g'} - \overline{w}\frac{\partial}{\partial r}\left(r\overline{\tilde{u}\tilde{w}}\right). \tag{A4}$$

Integrating these equations from $r = 0$ to ∞ taking as boundary conditions $\lim_{r\to\infty} r\ \overline{uw} = \lim_{r\to\infty} r\overline{\tilde{u}\tilde{w}} = \lim_{r\to\infty} r\overline{u}\overline{g'} = 0$, yields

$$\frac{\mathrm{d}}{\mathrm{d}z}\int_0^\infty r\overline{w}^2\mathrm{d}r = \int_0^\infty r\overline{g'}\mathrm{d}r, \tag{A5}$$

$$\frac{\mathrm{d}}{\mathrm{d}z}\int_0^\infty r\overline{w}\overline{g'}\mathrm{d}r = -\frac{\mathrm{d}\rho_a}{\mathrm{d}z}\frac{g}{\rho_r}\int_0^\infty r\overline{w}\mathrm{d}r, \tag{A6}$$

$$\frac{\mathrm{d}}{\mathrm{d}z}\int_0^\infty \frac{1}{2}r\overline{w}^3\mathrm{d}r = \int_0^\infty r\overline{w}\overline{g'}\mathrm{d}r + \int_0^\infty r\overline{\tilde{u}\tilde{w}}\frac{\partial \overline{w}}{\partial r}\mathrm{d}r. \tag{A7}$$

Three integral profiles are then used to define a top-hat,

$$R^2W^2 = \int_0^\infty r\overline{w}^2\mathrm{d}r, \tag{A8}$$

$$R^2G' = \int_0^\infty r\overline{g'}\mathrm{d}r, \tag{A9}$$

$$R^2WG' = \int_0^\infty r\overline{w}\overline{g'}\mathrm{d}r. \tag{A10}$$

Introducing three shape functions for velocity, buoyancy and turbulent shear stress,

$$\overline{w}(r,z) = w_m(z)f(r,z), \tag{A11}$$

$$\overline{g'}(r,z) = g'_m(z)h(r,z), \tag{A12}$$

$$\overline{\tilde{u}\tilde{w}}(r,z) = -\frac{1}{2}w_m(z)^2 j(r,z). \tag{A13}$$

Six integral profiles appear in the conservation equation,

$$I_1 = \int_0^\infty r^* f(r^*,z)h(r^*,z)\mathrm{d}r^*, \tag{A14}$$

$$I_2 = \int_0^\infty r^* h(r^*,z)\mathrm{d}r^*, \tag{A15}$$

$$I_3 = \int_0^\infty r^* f(r^*,z)^2\mathrm{d}r^*, \tag{A16}$$

$$I_4 = \int_0^\infty r^* f(r^*,z)^3\mathrm{d}r^*, \tag{A17}$$

$$I_5 = \int_0^\infty r^* j(r^*,z)\frac{\partial f}{\partial r^*}\mathrm{d}r^*, \tag{A18}$$

$$I_6 = \int_0^\infty r^* f(r^*,z)\mathrm{d}r^*, \tag{A19}$$

The resulting top-hat equations consistent with *Morton et al.* [1956] are

$$\frac{\mathrm{d}}{\mathrm{d}z}R^2W = 2RW\left[\mathrm{Ri}\left(1-\frac{1}{A}\right) + \frac{R}{2}\frac{\mathrm{d}\ln A}{\mathrm{d}z} + \frac{C}{2}\right], \tag{A20}$$

$$\frac{\mathrm{d}}{\mathrm{d}z}R^2W^2 = R^2G', \tag{A21}$$

$$\frac{\mathrm{d}}{\mathrm{d}z}R^2WG' = -E\frac{g}{\rho_r}\frac{\mathrm{d}\rho_a}{\mathrm{d}z}R^2W, \tag{A22}$$

where A, C and E are the following combinations of integral profiles,

$$A = \frac{I_2 I_4}{I_1 I_3}, \tag{A23}$$

$$C = \frac{I_2 I_3^{0.5} I_5}{I_1 I_4}, \tag{A24}$$

$$E = \frac{I_1 I_6}{I_2 I_3}. \tag{A25}$$

Parameters A and C have been constrained in our study, and E can be rewritten $4/(3A)$ which is close to 1. In our model we used $E = 1$ and checked that the results do not differ when using $4/(3A)$. In this new formalism, α_e is explicitly given as

$$\frac{C}{2} + \mathrm{Ri}\left(1 - \frac{1}{A}\right) + \frac{R}{2}\frac{\mathrm{d}\ln A}{\mathrm{d}z}. \tag{A26}$$

Appendix B: Theoretical Model of a Submarine Plume

[46] The model of *Rudnicki and Elderfield* [1992] is inspired by the work of *Morton et al.* [1956]. The conservation equations for the mass, the salt, the temperature and the momentum are,

$$\frac{\mathrm{d}Q}{\mathrm{d}z} = 2\alpha_e M^{1/2}, \tag{B1}$$

$$\frac{\mathrm{d}}{\mathrm{d}z}(S_a Q) = \frac{\mathrm{d}Q}{\mathrm{d}z} S_{a_e}, \tag{B2}$$

$$\frac{\mathrm{d}}{\mathrm{d}z}(TQ) = \frac{\mathrm{d}Q}{\mathrm{d}z} T_e, \tag{B3}$$

$$\frac{\mathrm{d}M}{\mathrm{d}z} = \frac{FQ}{M}, \tag{B4}$$

where S_a is the salinity, T the temperature and the subscript e denotes environmental conditions. The model assumes that the plume temperature and salinity only evolve by dilution with the entrained oceanic fluid. The temperature and the salinity are considered separately in order to calculate the density of the plume [*Speer and Rona*, 1989],

$$\rho = 1.041548 - 2.13 \times 10^{-4}(T - T_e) + 7.5 \times 10^{-4}(S - S_e). \tag{B5}$$

As the effect of salt variations at high temperature is unknown, the model does not account for it.

[47] **Acknowledgments.** The authors thank L.S. Glaze, L. Wilson, and an anonymous reviewer for constructive comments.

References

Abraham, G., and W. D. Eysink (1969), Jets issuing into fluids with a density gradient, *Delft. Hydr. Lab. Publ.*, *66*, 145–175.

Baines, W. D. (1983), A technique for the direct measurement of volume flux of a plume, *J. Fluid. Mech.*, *132*, 247–256.

Bischoff, J. L., and R. J. Rosenbauer (1985), An empirical equation of state for hydrothermal seawater (3.2 percent NaCl), *Amer. J. Sci.*, *285*, 725–763.

Bloomfield, L. J., and R. C. Kerr (2000), A theoretical model of a turbulent fountain, *J. Fluid. Mech.*, *424*, 197–216.

Bonadonna, C., and J. C. Phillips (2003), Sedimentation from strong volcanic plumes, *J. Geophys. Res.*, *108*(B7), 2340, doi:10.1029/2002JB002034.

Bonadonna, C., J. C. Phillips, and B. F. Houghton (2005), Modeling tephra sedimentation from a Ruapehu weak plume eruption, *J. Geophys. Res.*, *110*, B08209, doi:10.1029/2004JB003515.

Borisova, A. Y., M. Pichavant, J.-M. Beny, O. Rouer, and J. Pronost (2005), Constraints on dacite magma degassing and regime of the June 15, 1991, climatic eruption of Mount Pinatubo (Philippines): New data on melt and crystal inclusions in quartz, *J. Volcanol. Geotherm. Res.*, *145*, 35–67.

Briggs, G. A. (1969), Optimum formulas for buoyant plume rise, *Philos. Trans. R. Soc. Lond.*, *265*, 197–203.

Bursik, M. (2001), Effect of wind on the rise height of volcanic plumes, *Geophys. Res. Lett.*, *28*, 3621–3624.

Bursik, M., S. Carey, R. S. J. Sparks, and J. Gilbert (1992), Sedimentation of tephra by volcanic plumes: I. Theory and its comparison with a study of the Fogo A Plinian deposit, Sao Miguel (Azores), *Bull. Volcanol.*, *54*, 329–334.

Carazzo, G., E. Kaminski, and S. Tait (2006), The route to self-similarity in turbulent jets and plumes, *J. Fluid. Mech.*, *547*, 137–148.

Carazzo, G., E. Kaminski, and S. Tait (2008), On the dynamics of volcanic columns: A comparison of field data with a new model of negatively buoyant jets, *J. Volcanol. Geotherm. Res.*, doi:10.1016/j.jvolgeores.2008.01.002.

Carey, S., and H. Sigurdsson (1985), The May 18, 1980 eruption of Mount St. Helens: 2. Modeling of dynamics of the Plinian phase, *J. Geophys. Res.*, *90*, 2948–2958.

Carey, S., and H. Sigurdsson (1989), The intensity of Plinian eruptions, *Bull. Volcanol.*, *51*, 28–40.

Carey, S., and R. S. J. Sparks (1986), Quantitative models of the fallout and dispersal of tephra from volcanic eruption columns, *Bull. Volcanol.*, *48*, 109–125.

Carey, S., H. Sigurdson, J. E. Gardner, and W. Criswell (1990), Variations in column height and magma discharge during the May 18, 1980 eruption of Mount St. Helens, *J. Volcanol. Geotherm. Res.*, *43*, 99–112.

Caulfield, C. P., and A. W. Woods (1998), Turbulent gravitational convection from a point source in a non-uniformly stratified environment, *J. Fluid Mech.*, *360*, 229–248.

Chen, J. C., and W. Rodi (1980), Vertical turbulent buoyant jets - a review of experimental data, Pergamon Press, New York.

Chesser, R. K., M. Bondarkov, R. J. Baker, J. K. Wickliffe, and B. E. Rodgers (2004), Reconstruction of radioactive plume characteristics along Chernobyl's Western Trace, *J. Environ. Radioact.*, *71*, 147–157.

Connor, C. B., L. Powell, W. Strauch, M. Navarro, O. Urbina, and W. I. Rose (1993), The 1992 eruption of Cerro Negro, Nicaragua: An example of Plinian-style activity at a small basaltic cinder cone, *EOS Trans.*, *74*, 640.

Crawford, T. V., and A. S. Leonard (1962), Observations of buoyant plumes in calm stably air, *J. Appl. Meteorol.*, *1*, 251–256.

Dash, S. M., D. E. Wolf, R. A. Beddini, and H. S. Pergament (1985), Analysis of two-phase processes in rocket exhaust plumes, *J. Spacecr. Rockets*, *22*, 367–380.

Davies, R. W. (1969), Large scale diffusion from an oil fire, *Adv. Geophys.*, *6*, 413–415.

Di Muro, A., A. Neri, and M. Rosi (2004), Contemporaneous convective and collapsing eruptive dynamics: The transitional regime of explosive eruptions, *Geophys. Res. Lett.*, *31*, l10607, doi:10.1029/2004GL019709.

Ernst, G. G. J., R. S. J. Sparks, S. N. Carey, and M. I. Bursik (1996), Sedimentation from turbulent jets and plumes, *J. Geophys. Res.*, *101*, 5575–5589.

Esposito, L. W. (1984), Sulfur dioxide: Episodic injection shows evidence for active Venus volcanism, *Science*, *223*, 1072–1074.

Fan, L. (1967), Turbulent buoyant jets into stratified or flowing ambient fluids, *Report KH-R-15*, California Inst. of Technology, Pasadena, California, USA.

Fischer, H. B., E. J. List, R. C. Y. Koh, J. Imberger, and N. H. Brooks, (Eds.) (1979), *Mixing in Inland and Coastal Waters*, Academic, New-York.

Folch, A., and A. Felpeto (2005), A coupled model for dispersal of tephra during sustained explosive eruptions, *J. Volcanol. Geotherm. Res.*, *145*, 337–349.

Fox, D. G. (1970), Forced plume in a stratified fluid, *J. Geophys. Res.*, *33*, 6818–6835.
Glaze, L. S. (1999), Transport of SO_2 by explosive volcanism on Venus, *J. Geophys. Res.*, *104*, 18,899–18,906.
Glaze, L. S., and S. M. Baloga (1996), Sensitivity of buoyant plume heights to ambient atmospheric conditions: Implications for volcanic eruption columns, *J. Geophys. Res.*, *101*, 1529–1540.
Glaze, L. S., and S. M. Baloga (2002), Volcanic plume heights on Mars: Limits of validity for convective models, *J. Geophys. Res.*, *107*(E10), 5086, doi:10.1029/2001JE001830.
Glaze, L., S. M. Baloga, and L. Wilson (1997), Transport of atmospheric water vapor by volcanic eruption columns, *J. Geophys. Res.*, *102*, 6099–6108.
Hart, W. E. (1961), Jet discharge into a fluid with a density gradient, *Proc. Am. Soc. Civ. Eng.*, *87*, 171–200.
Holasek, R. E., S. Self, and A. W. Woods (1996), Satellite observation and interpretation of the 1991 Mount Pinatubo eruption plumes, *J. Geophys. Res.*, *101*, 27,635–27,655.
Hornwell, C. J. (2007), Grain-size analysis of volcanic ash for the rapid assessment of respiratory health hazard, *J. Environ. Monit.*, *9*, 1107–1115.
Hort, M., and C. M. Weitz (2001), Theoretical modeling of eruption plumes on Mars under current and past climates, *J. Geophys. Res.*, *106*, 20,547–20,562.
Hunt, G. R., and N. G. Kaye (2001), Virtual origin correction for lazy turbulent plumes, *J. Fluid. Mech.*, *435*, 377–396.
Ishimine, Y. (2006), Sensitivity of the dynamics of volcanic eruption columns to their shape, *Bull. Volcanol.*, *68*, 516–537.
Ishimine, Y. (2007), A simple integral model of buoyancy-generating plumes and its application to volcanic eruption columns, *J. Geophys. Res.*, *112*, B03210, doi:10.1029/2006JB004274.
Kaminski, E., S. Tait, and G. Carazzo (2005), Turbulent entrainment in jets with arbitrary buoyancy, *J. Fluid Mech.*, *526*, 361–376.
Kieffer, S. W. (1995), Numerical models of caldera-scale volcanic eruptions on Earth, Venus, and Mars, *Science*, *269*, 1385–1391.
Koyaguchi, T., and M. Ohno (2001), Reconstruction of eruption column dynamics on the basis of grain size of tephra fall deposits: 2. Application to the Pinatubo 1991 eruption, *J. Geophys. Res.*, *106*, 6513–6533.
Kusanagi, T., and T. Matsui (2000), The change of eruption styles of Martian volcanoes and estimates of the water content of the Martian mantle, *Earth Planet. Sci. Lett.*, *117*, 437–447.
List, E. J. (1982), Turbulent jets and plumes, *Ann. Rev. Fluid Mech.*, *14*, 189–212.
Luhr, J. (1990), Experimental phase relations of water- and sulfur-saturated arc magmas and the 1982 eruptions of El Chichon volcano, *J. Petrol.*, *31*, 1071–1114.
Lupton, J. E., E. T. Baker, and G. J. Massoth (1989), Variable ^{3}He/heat ratio in submarine hydrothermal systems: Evidence from two plumes over the Juan de Fuca ridge, *Nature*, *337*, 161–164.
Manins, P. C. (1985), Cloud heights and stratospheric injections resulting from a thermonuclear war, *Atmos. Environ.*, *19*, 1245–1255.
Morton, B. R. (1959), Forced plumes, *J. Fluid Mech.*, *5*, 151–163.
Morton, B. R., G. I. Taylor, and J. S. Turner (1956), Turbulent gravitational convection from maintained and instantaneous source, *Proc. R. Soc. Lond.*, *234*, 1–23.
Neri, A., and F. Dobran (1994), Influence of eruption parameters on the thermofluid dynamics of collapsing volcanic columns, *J. Geophys. Res.*, *99*, 11,833–11,857.
Neri, A., T. Esposti Ongaro, G. Menconi, M. De'Michieli Vitturi, C. Cavazzoni, G. Erbacci, and P. J. Baxter (2007), 4D simulation of explosive dynamics at Vesuvius, *Geophys. Res. Lett.*, *34*, L04309, doi:10.1029/2006GL028597.
Neuville, D. R., P. Courtial, D. B. Dingwell, and P. Richet (1993), Thermodynamic and rheological properties of rhyolite and andesite melts, *Contrib. Miner. Petrol.*, *113*, 572–581.
Nielsen, P. V. (1993), Displacement ventilation — theory and design, Ph.D. thesis, Aalborg University, Aalborg, Denmark.
Oberhuber, J. M., M. Herzog, H.-F. Graf, and K. Schwanke (1998), Volcanic plume simulation on large scales, *J. Volcanol. Geotherm. Res.*, *87*, 29–53.
Papanicolaou, P. N., and E. J. List (1988), Investigations of round vertical turbulent buoyant jets, *J. Fluid Mech.*, *195*, 341–391.
Priestley, C. H. B., and F. K. Ball (1955), Continuous convection from an isolated source of heat, *Q. J. R. Met. Soc.*, *81*, 144–157.
Ramondenc, P., L. N. Germanovich, K. L. V. Damm, and R. P. Lowell (2006), The first measurements of hydrothermal heat output at 9°50′N, East Pacific Rise, *Earth Planet. Sci. Lett.*, *245*, 487–497.
Rampino, M. R., and S. Self (1984), The atmospheric effects of El Chichon, *Sci. Amer.*, *250*, 48–57.
Robinson, C. A., G. D. Thornhill, and E. A. Parfitt (1995), Large-scale volcanic activity at Maas Mons: Can this explain fluctuations in atmospheric chemistry observed by Pioneer Venus?, *J. Geophys. Res.*, *100*, 11,755–11,763.
Roggensack, K., R. L. Hervig, S. B. McKnight, and S. N. Williams (1997), Explosive basaltic volcanism from Cerro Negro volcano: Influence of volatiles on eruptive style, *Science*, *277*, 1639–1642.
Rudnicki, M. D., and H. Elderfield (1992), Theory applied to the Mid-Atlantic Ridge hydrothermal plumes: The finite-difference approach, *J. Volcanol. Geotherm. Res.*, *50*, 161–172.
Rutherford, M., H. Sigurdsson, S. Carey, and A. Davis (1985), The May 18, 1980 eruption of Mount St. Helens: 1. Melt composition and experimental phase equilibria, *J. Geophys. Res.*, *90*, 2929–2947.
Seiff, A., and D. B. Kirk (1977), Structure of the atmosphere of Mars in summer at midlatitudes, *J. Geophys. Res.*, *82*, 4364–4378.
Settle, M. (1978), Volcanic eruption clouds and the thermal power output of explosive eruptions, *J. Volcanol. Geotherm. Res.*, *3*, 309–324.
Sigurdsson, H., S. Carey, and R. V. Fisher (1987), The 1982 eruption of El Chichon volcano, Mexico (3): Physical properties of pyroclastic surges, *Bull. Volcanol.*, *49*, 467–488.
Sinha, N., D. C. Kenzakowski, J. Papp, and B. J. York (2002), Particulate dispersion in rocket exhaust plumes, *38th AIAA ASME SAE ASEE Joint Propulsion Conference and Exhibit*, Paper AIAA 2002-4289.
Sneck, H. J., and D. H. Brown (1974), Plume rise from large thermal sources such as dry cooling towers, *ASME J. Heat Trans.*, 232–238.
Sparks, R. S. J. (1986), The dimensions and dynamics of volcanic eruption columns, *Bull. Volcanol.*, *48*, 3–15.
Sparks, R. S. J., and L. Wilson (1976), A model for the formation of ignimbrite by gravitational column collapse, *J. Geol. Soc. Lond.*, *132*, 441–451.
Sparks, R. S. J., M. I. Bursik, G. J. Ablay, R. M. E. Thomas, and S. N. Carey (1992), Sedimentation of tephra by volcanic plumes: part II. Controls on thickness and grain-size variations of tephra fall deposits, *Bull. Volcanol.*, *54*, 685–695.
Sparks, R. S. J., M. Bursik, S. Carey, J. S. Gilbert, L. S. Glaze, H. Sigurdsson, and A. W. Woods (Eds.) (1997), *Volcanic Plumes*, John Wiley, New York.
Speer, K. G., and P. A. Rona (1989), A model of an Atlantic and Pacific hydrothermal plume, *J. Geophys. Res.*, *94*, 6213–6220.
Squyres, S. W., and J. F. Kasting (1994), Early Mars: How warm and how wet?, *Science*, *265*, 744–749.
Suzuki, Y. J., T. Koyaguchi, M. Ogawa, and I. Hachisu (2005), A numerical study of turbulent behavior in eruption clouds using a 3-D fluid-dynamics model, *J. Geophys. Res.*, *110*, B08201, doi:10.1029/2004JB003460.
Thornhill, G. D. (1993), Theoretical modeling of eruption plumes on Venus, *J. Geophys. Res.*, *98*, 9107–9111.
Trentmann, J., G. Luderer, T. Winterrath, R. Servranckx, C. Textor, M. Herzog, H.-F. Graf, and M. O. Andrae (2006), Modeling of biomass smoke injection into the lower stratosphere by a large forest fire (Part I): Reference simulation, *Atmos. Chem. Phys.*, *6*, 5247–5260.
Valentine, G. A., and K. H. Wohletz (1989), Numerical models of Plinian eruption columns and pyroclastic flows, *J. Geophys. Res.*, *94*, 1867–1887.
Varekamp, J. C., J. F. Luhr, and K. L. Prestegaard (1984), The 1982 eruption of El Chichon volcano (Chiapas, Mexico): Character of the eruptions, ash-fall deposits and gas phase, *J. Volcanol. Geotherm. Res.*, *23*, 39–68.
Vehrencamp, J. E., A. Ambrosio, and F. E. Romie (1955), *Convection From Heated Sources in an Inversion Layer*, pp. 55–27, Univ. of California, Los Angeles, Department of Engineering, Los Angeles, California, USA.
Veitch, G., and A. W. Woods (2000), Particle recycling and oscillations of volcanic eruption columns, *J. Geophys. Res.*, *105*, 2829–2842.
Veitch, G., and A. W. Woods (2002), Particle recycling in volcanic plumes, *Bull. Volcanol.*, *64*, 31–39.
Wallace, P. J. (2005), Volatiles in subduction zone magmas: Concentrations and fluxes based on melt inclusion and volcanic gas data, *J. Volcanol. Geotherm. Res.*, *140*, 217–240.
Wang, H., and A. W.-K. Law (2002), Second-order integral model for a round turbulent buoyant jet, *J. Fluid Mech.*, *459*, 397–428.
Wilson, L. (1976), Explosive volcanic eruptions: III. Plinian eruption columns, *J. R. Astron. Soc.*, *45*, 543–556.
Wilson, L., and J. W. Head (1983), A comparison of volcanic eruption processes on Earth, Moon, Mars, Io and Venus, *Nature*, *302*, 663–669.
Wilson, L., and J. W. Head (1994), Mars: Review and analysis of volcanic eruption theory and relationships to observed landforms, *Rev. Geophys.*, *32*, 221–263.
Wilson, L., and G. P. L. Walker (1987), Explosive volcanic eruptions: VI. Ejecta dispersal in Plinian eruptions: The control of eruption conditions and atmospheric properties, *Geophys. J. R. Astron. Soc.*, *89*, 657–679.
Wilson, L., R. S. J. Sparks, T. C. Huang, and N. D. Watkins (1978), The control of volcanic column heights by eruption energetics and dynamics, *J. Geophys. Res.*, *83*, 1829–1836.

Wilson, L., R. S. J. Sparks, and G. P. L. Walker (1980), Explosive volcanic eruptions: IV. The control of magma properties and conduit geometry on eruption column behaviour, *Geophys. J. R. Astron. Soc.*, *63*, 117–148.

Woods, A. W. (1988), The fluid dynamics and thermodynamics of eruption columns, *Bull. Volcanol.*, *50*, 169–193.

Woods, A. W. (1993), Moist convection and the injection of volcanic ash into the atmosphere, *J. Geophys. Res.*, *98*, 17,627–17,636.

Woods, A. W. (1995), The dynamics of explosive volcanic eruptions, *Rev. Geophys.*, *33*, 495–530.

Woods, A. W. (1998), Observations and models of volcanic eruption columns, *Geol. Soc. Lond. Spec. Publ.*, *145*, 91–114.

Woods, A. W., and S. M. Bower (1995), The decompression of volcanic jets in a crater during explosive volcanic eruptions, *Earth Planet. Sci. Lett.*, *131*, 189–205.

Woods, A. W., and M. Bursik (1991), Particle fallout, thermal disequilibrium and volcanic plumes, *Bull. Volcanol.*, *53*, 559–570.

Woods, A. W., and C. P. Caulfield (1992), A laboratory study of explosive volcanic eruptions, *J. Geophys. Res.*, *97*, 6699–6712.

G. Carazzo, E. Kaminski, and S. Tait, Equipe de Dynamique des Fluides Géologiques, IPG Paris, 4 Place Jussieu, 75 052 Paris Cédex 05, France. (carazzo@ipgp.jussieu.fr; kaminski@ipgp.jussieu.fr; tait@ipgp.jussieu.fr)